

Master thesis submitted for the degree *Candidata pharmaciae*

COMPARISON OF THREE *IN VITRO* MODELS EXPRESSING THE MEMBRANE DRUG TRANSPORTER OATP1B1



Maria Ulvestad

Department of Pharmaceutical Biosciences,
School of Pharmacy,
Faculty of Mathematics and Natural Sciences,
University of Oslo, Norway

December 2007

AstraZeneca 

COMPARISON OF THREE *IN VITRO* MODELS EXPRESSING THE MEMBRANE DRUG TRANSPORTER OATP1B1

Master thesis submitted to
Department of Pharmaceutical Biosciences, School of Pharmacy,
Faculty of Mathematics and Natural Sciences, University of Oslo
for the degree candidata pharmaciae

Maria Ulvestad

Supervisors:

Associate professor Tommy B. Andersson, Ph.D.

Development DMPK & Bioanalysis, AstraZeneca R&D Mölndal

Johan E. Karlsson, Ph.D.

Development DMPK & Bioanalysis, AstraZeneca R&D Mölndal

Espen Molden, Ph.D.

Department of Pharmaceutical Biosciences, School of Pharmacy, University of Oslo

Professor Anders Åsberg, Ph.D.

Department of Pharmaceutical Biosciences, School of Pharmacy, University of Oslo

December 2006 – December 2007

Experimental DMPK, Development DMPK & Bioanalysis, AstraZeneca

R&D Mölndal, Sweden



ACKNOWLEDGEMENTS

First of all, I would like to thank Espen Molden for excellent supervision including inspiring discussions, creative ideas, and invaluable help during the process of writing. I am also grateful that you made the cooperation with AstraZeneca Mölndal possible.

I would like to thank Tommy B. Andersson for the opportunity to perform my Master of Pharmacy project at Development DMPK & Bioanalysis. Thank you for valuable discussions and ideas, and for your interest in my work.

Furthermore, I would like to thank Johan E. Karlsson for frequent supervision, for taking care of all practical matters, and for a helping hand in the laboratory.

I would like to thank Malin Forsgard for guidance and help in the laboratory, and for all practical assistance.

Thank you, Malin Darnell, for a helping hand and an encouraging word in every situation. Thank you for guidance in the laboratory, and for valuable discussions of all kinds.

Thanks to Linn Kihlgren for the help in seeding and feeding my cells.

I am also thankful to everyone at Experimental DMPK, and other colleagues I have learned to know at AstraZeneca Mölndal, for being friendly and supportive at all times.

Finally, I would like to thank my outstanding family and friends for support, interest, and encouragement whenever needed. I wouldn't have made it without you. Thank you!

Mölndal, December 2007

Maria Ulvestad

TABLE OF CONTENTS

ABBREVIATIONS	6
ABSTRACT	7
1 INTRODUCTION	9
1.1 Background	9
1.2 Membrane transporter families	10
1.2.1 The OATP family.....	10
1.2.2 OATP1B1	10
1.3 HMG-CoA reductase inhibitors	12
1.3.1 Pravastatin	13
1.3.2 Atorvastatin	15
1.4 <i>In vitro</i> transport systems	16
1.4.1 HEK293 cells	17
1.4.2 <i>Xenopus laevis</i> oocytes	17
1.4.3 HepaRG cells.....	17
1.5 Transport kinetics	17
1.6 Purpose of the study	19
2 MATERIALS AND METHODS	20
2.1 Materials	20
2.2 Cell culturing and seeding	20
2.2.1 HEK 293 cells	20
2.2.2 HepaRG cells.....	22
2.3 Preperation of <i>Xenopus laevis</i> oocytes	22
2.4 Transport experiments with HEK293 cells and HepaRG cells	23
2.4.1 Preparation of buffer solution and test solutions	23
2.4.2 Uptake experiments with HEK293 cells.....	23
2.4.3 Uptake experiments with HepaRG cells	24
2.5 Transport experiments with <i>Xenopus laevis</i> oocytes	25
2.5.1 Preparation of buffer solution and test solutions	25
2.5.2 Uptake experiments with oocytes.....	25
2.6 Analysis	26
2.6.1 Liquid scintillation counting	26
2.6.2 Protein quantification	27
2.6.3 mRNA quantification	27
2.7 Data analysis	28
3 RESULTS	29
3.1 Time dependence uptake studies	29
3.1.1 HEK293 cells	29
3.1.2 Hepa RG cells.....	31
3.1.3 <i>Xenopus laevis</i> oocytes	33
3.2 Concentration dependence uptake studies	36
3.2.1 HEK293 cells	36
3.2.2 HepaRG cells.....	39
3.2.3 <i>Xenopus laevis</i> oocytes	41
3.3 mRNA quantification	44
4 DISCUSSION	45
4.1 Methodological considerations	45
4.2 Transport studies	46

5	SUMMARY AND CONCLUSION	49
6	REFERENCES	50
7	APPENDIX.....	57
7.1	Appendix 1	57
7.2	Appendix 2	58
7.3	Appendix 3	61
7.4	Appendix 4	65

ABBREVIATIONS

ABC	ATP-binding cassette (transporter family)
AUC	Area under the plasma concentration-time profile
ATP	Adenosine triphosphate
BCRP	Breast cancer resistance protein
BSA	Bovine serum albumin
BSEP	Bile salt exporting pump
cRNA	Complementary ribonucleic acid
CYP	Cytochrome P450
DMSO	Dimethylsulfoxide
E17βG	Estradiol-17 β -D-glucuronide
EDTA	Ethylene diamine tetraacetic acid
FBS/FCS	Foetal bovine serum/foetal calf serum
HBSS	Hank's balanced salt solution
HEK293 cells	Human embryonic kidney cells
HEK293/OATP1B1	Human embryonic kidney cells transfected with the gene encoding OATP1B1
HEK293/pT-REX	Human embryonic kidney cells transfected with the empty vector pT-REX
HEPES	2-[4-(2-hydroxyethyl)-1-piperazinyl]ethanesulfonic acid
HMG-CoA	3-hydroxy-3-methylglutaryl coenzyme A
IC₅₀	Inhibitor concentration to produce a 50% reduction
K_i	Inhibition constant
K_m	Michaelis constant
LDL	Low density lipoprotein
LogD	The logarithm of the distribution coefficient
MDR	Multidrug resistance
mRNA	Messenger ribonucleic acid
MRP	Multidrug resistance associated protein
MVP	Major vault protein
OATP	Organic anion transporting polypeptide
P-gp	P-glycoprotein
PPIA	Peptidylprolyl isomerase A
RT-PCR	Real time-polymerase chain reaction
SDS	Sodium dodecyl sulfate
SLC	Solute carrier (transporter family)
V₀	Initial velocity
V_{max}	Maximum velocity

ABSTRACT

Background: Drug transporters have been increasingly recognized as important determinants of variable drug disposition and response. For the pharmaceutical industry it is of importance to develop *in vitro* models, which could predict possible transporter-associated genetic variability and drug-drug interactions of a new compound. The purpose of this study was to compare uptake kinetics of estradiol-17 β -D-glucuronide, atorvastatin and pravastatin in three *in vitro* models expressing the membrane drug transporter OATP1B1.

Methods: Two *in vitro* models overexpressing OATP1B1 were applied in this study; HEK293 cells transfected with the gene encoding OATP1B1 and *Xenopus laevis* oocytes injected with OATP1B1 cDNA. HEK293 cells transfected with the empty vector pT-REX and water injected oocytes were used as control systems. HepaRG cells, the third model applied in this study, express naturally occurring levels of OATP1B1 and other transporters, and studies at 4°C were used as control. Uptake studies were performed with three known substrates for OATP1B1; estradiol-17 β -D-glucuronide, atorvastatin and pravastatin. Time- and concentration dependent uptake was studied. K_m values were estimated by non-linear regression analysis of the active uptake calculated in concentration dependence studies. The active uptake was calculated as the difference between intrasystemic accumulation of test substance in the model system and in the respective control system.

Results: Estradiol-17 β -D-glucuronide exhibited active uptake in all time- and concentration dependence uptake studies performed on the three models. The active transport of estradiol-17 β -D-glucuronide was saturated in the concentration dependence studies, with estimated K_m values of $5.6 \pm 0.3 \mu\text{M}$, $5.9 \pm 3.8 \mu\text{M}$ and $22.3 \pm 7.1 \mu\text{M}$ in HEK293 cells, oocytes and HepaRG cells, respectively. Atorvastatin showed active uptake in all time dependence uptake studies. In the concentration dependence uptake studies, atorvastatin exhibited no active uptake in HEK293 cells and oocytes, while in the HepaRG cells, a non-saturated active uptake was demonstrated. In the time dependence uptake studies with pravastatin, an active uptake was shown in HEK293 and HepaRG cells, while a limited active uptake was demonstrated in the oocytes. On the contrary, concentration dependence uptake studies showed no active uptake of pravastatin in HEK293 and HepaRG cells, but a saturated active uptake in oocytes with estimated K_m value of $54.8 \pm 31.4 \mu\text{M}$.

Discussion and conclusion: Estradiol-17 β -D-glucuronide was the only substrate showing consistent time- and concentration dependent results in all tested models. Results from the studies with atorvastatin and pravastatin were inconsistent between the models. Furthermore, concentration dependence and saturation of uptake was difficult to obtain even if a time dependent uptake was recorded. The inconsistent results with atorvastatin and pravastatin could be due to the higher lipophilicity and greater extent of passive diffusion compared to

estradiol-17 β -D-glucuronide. It could therefore be hypothesized that when a substrate exhibits greater passive diffusion than active uptake, the models would not be sufficiently sensitive to separate the active uptake from the passive uptake. As drugs are generally more lipophilic than estradiol-17 β -D-glucuronide, none of the *in vitro* transport models studied are expected to be appropriate for routine screening of new drugs as possible substrates for OATP1B1.

1 INTRODUCTION

1.1 Background

Pharmacokinetics refers to the processes of drug absorption, distribution, metabolism and elimination, while pharmacodynamic processes involve the mechanisms of drug action. Drug efficacy reflects the interplay of pharmacokinetics and pharmacodynamics (Buxton, 2006).

In drug development, it is of importance to reveal which pharmacokinetic processes that determine the systemic drug exposure. Most studies to date have focused on metabolizing enzymes and filtration in the kidneys as pharmacokinetic variables causing interindividual differences in drug exposure (Gonzales and Tukey, 2006). Drug-metabolizing reactions are classified into phase I and phase II. Phase I reactions involves oxidation, reduction or hydrolysis of the drug, and are primarily mediated by the cytochrome P450 family of enzymes. Phase II reactions involve covalently binding of an endogenous compound, most often glucuronide acid, glutathione or sulfate, to the phase I-metabolite. This conjugation produces a more polar metabolite and promotes excretion of the drug (Gonzales and Tukey, 2006; Ho and Kim, 2005).

Most pharmacokinetic processes involve drug passage across cell membranes, even metabolism. Drugs require transport into intestine and/or liver cells, to be susceptible to metabolism. Physiochemical properties of a drug that determine its movement and access to target tissue are molecular size and shape, pK_a , lipophilicity and binding to serum and tissue proteins. Passive diffusion through the membrane has been viewed as dominant in the disposition of most drugs (Buxton, 2006), but it is now increasingly recognized that carrier-mediated transport have a significant impact on the absorption, distribution and elimination of the drug (Ho and Kim, 2005; Kim, 2006; Ware, 2006; Yamazaki et al., 2005). Interindividual variability in carrier-mediated transport, due to inheritable differences in the genes encoding specific transporters or drug-drug interactions, may be an important cause of abnormal drug exposure and response.

For the pharmaceutical industry it is of importance to develop *in vitro* models, which could predict possible genetic variability and drug-drug interactions of a new compound associated to active transport. A transporter of particular interest is the organic anion transporting polypeptide 1B1 (OATP1B1), which is located in the blood-liver interface and believed to be important in hepatic clearance of several drugs (Lau et al., 2004; Sasaki et al., 2004; Smith et al., 2005; Yamazaki et al., 1996).

1.2 Membrane transporter families

Two major gene superfamilies play a prominent role in the transport of drugs across biological membranes; the solute carrier (SLC) superfamily and the ATP-binding cassette (ABC) superfamily (Giacomini and Sugiyama, 2006). The members of the SLC superfamily are uptake transporters, and the most important subfamilies involved in disposition of drugs are the organic anion transporting polypeptide (OATP) family, the organic anion transporter (OAT) family and the organic cation transporter (OCT) family (Kim, 2006). The members of the ABC superfamily are efflux transporters, using energy released from ATP hydrolysis to transport substrates out of cells (Davidson and Maloney, 2007). The most important proteins involved in this transport are P-glycoprotein (P-gp/MDR-1), multidrug resistance associated protein 2 (MRP2), bile salt exporting pump (BSEP) and breast cancer resistance protein (BCRP) (Kim, 2006).

1.2.1 The OATP family

The human OATP family consists of 11 members, where all share a similar transmembrane domain organisation with 12 predicted domains (Figure 1.1) (Hagenbuch and Meier, 2004; Meier et al., 1997). The OATPs are expressed in multiple tissues, including the intestine, liver, kidney and brain, where they mediate the sodium-independent transport of a wide variety of substrates, i.e. bile salts, hormones and steroid conjugates (Abe et al., 1999; Kakyo et al., 1999; Konig et al., 2006).

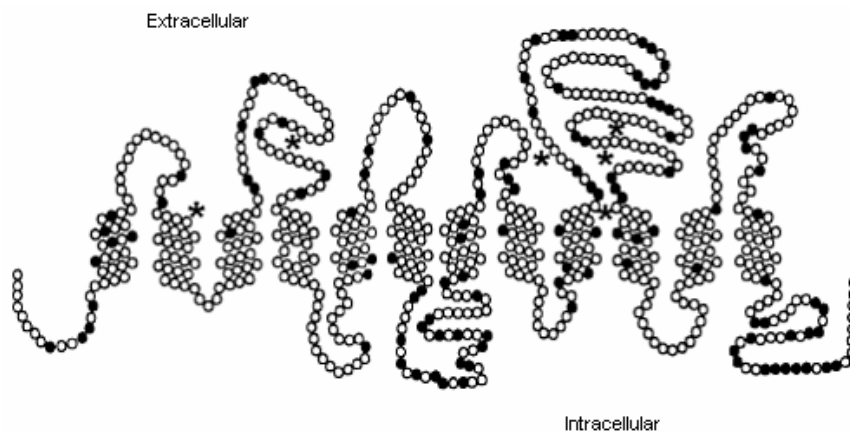


Figure 1.1 Structure of the OATP transporters which all consist of 670 amino acids with 12 putative transmembrane domains. All seven potential N-linked glycosylation sites are located on the same side of the membrane suggesting that both the N- and C-terminal of the protein are situated within inside the cell (Meier et al., 1997).

1.2.2 OATP1B1

OATP1B1 (formerly OATP-C, OATP2, LST-1; gene symbol *SLCO1B1*) belongs to the OATP1B subfamily of the OATP family. OATP1B1 is expressed primarily in the liver, and is localised primarily to the basolateral membrane of hepatocytes (Figure 1.3) (Hsiang et al., 1999; Konig et al., 2000). In the addition to transport of endogenous substances (e.g. bile salts, steroids, leukotriene C₄ and thyroid hormone), OATP1B1 is capable of transporting

various xenobiotics and drugs into hepatocytes, facilitating the hepatocellular accumulation of these substrates prior to metabolism and/or excretion into bile (Figure 1.3) (Hsiang et al., 1999). Estradiol-17 β -D-glucuronide (Figure 1.2) and estrone sulfate are extensively studied probe substrates for the OATP1B1 transporter (Iwai et al., 2004; Konig et al., 2000; Matsushima et al., 2005; Nakai et al., 2001; Nozawa et al., 2002; Sasaki et al., 2004; Sasaki et al., 2002).

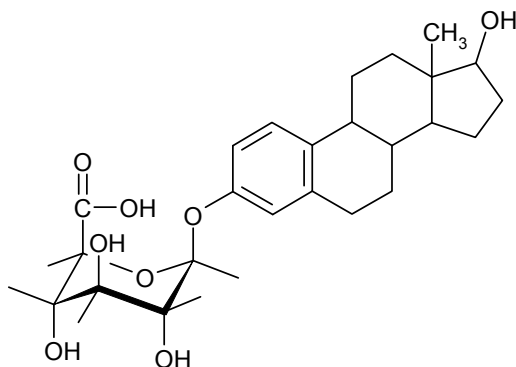


Figure 1.2 Chemical structure of estradiol-17 β -D-glucuronide.

Other OATP1B1 substrates include pravastatin (Hsiang et al., 1999; Nakai et al., 2001) and atorvastatin (Kameyama et al., 2005). Ciclosporine A, rifampicin and gemfibrozil have all been reported to inhibit the transport function of OATP1B1 *in vitro* (Nakagomi-Hagihara et al., 2007; Noe et al., 2007; Schneck et al., 2004; Shitara et al., 2004a; Shitara et al., 2004b; Tirona et al., 2003), introducing the risk of drug-drug interactions following co-administration with OATP1B1 substrates (Nakagomi-Hagihara et al., 2007; Noe et al., 2007; Schneck et al., 2004; Shitara et al., 2004a; Shitara et al., 2004b).

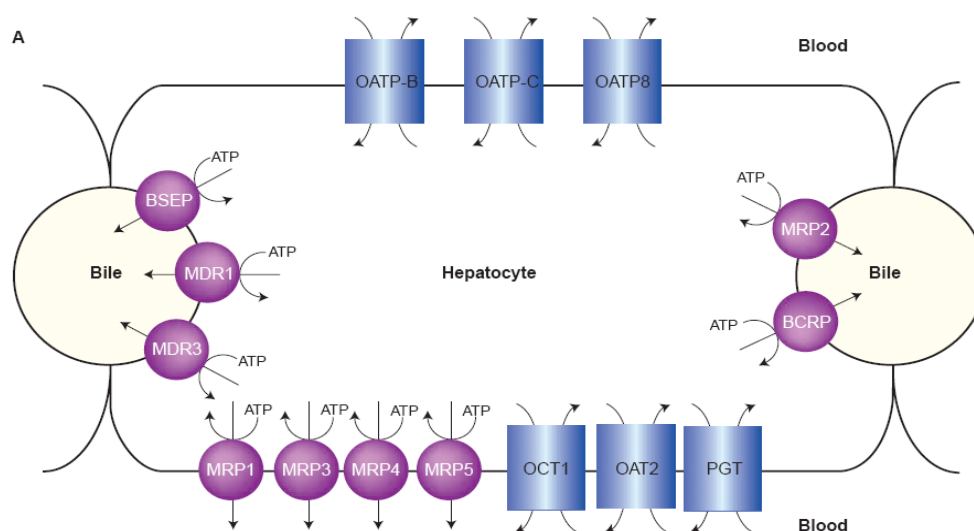


Figure 1.3 Uptake and efflux transporters and their localization in human hepatocytes (OATP1B1 is expressed by the former name OATP-C) (Marzolini et al., 2004).

Polymorphisms in genes encoding transport proteins may play an important role in the interindividual variability of drug disposition and drug response. A number of single nucleotide polymorphisms (SNPs) and haplotypes of *SLCO1B1* have been reported (Figure 1.4) (Michalski et al., 2002; Nishizato et al., 2003; Nozawa et al., 2002; Pasanen et al., 2006; Rohrbacher et al., 2006; Tirona et al., 2001).

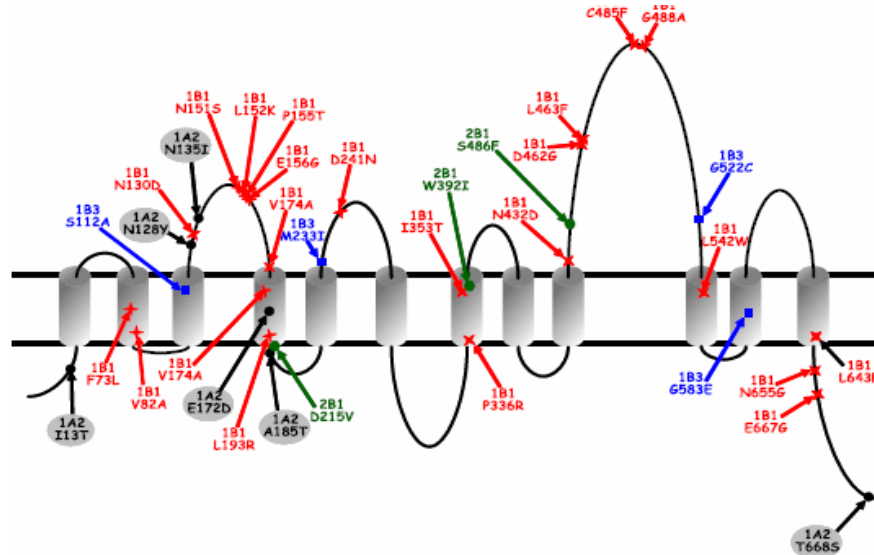


Figure 1.4 Localisation of amino acid exchanges caused by mutations in genes encoding human members of the OATP family. Mutations in the *SLCO1B1* gene encoding OATP1B1 are shown in red (Konig et al., 2006).

The SNP 521T>C is commonly existing in four major haplotypes of OATP1B1. Of these haplotypes, at least *5, *15 and *17 have been associated with increased plasma concentrations of various statins (Chung et al., 2005; Lee et al., 2005; Mwinyi et al., 2004; Niemi et al., 2004), suggesting that the 521T>C SNP determines the functional properties of these OATP1B1 haplotypes. At the molecular level, the reduced OATP1B1 transport function may be explained by defects in cell surface trafficking of the transporter protein (Kameyama et al., 2005; Tirona et al., 2001).

1.3 HMG-CoA reductase inhibitors

3-hydroxy-3-methylglutaryl coenzyme A (HMG-CoA) reductase inhibitors (statins) are widely used lipid-lowering drugs. Statins inhibit the synthesis of mevalonate in hepatocytes, the rate-limiting step in cholesterol biosynthesis, leading to a reduction in the plasma low density lipoprotein (LDL)-cholesterol level. High plasma LDL-cholesterol is a risk factor of cardiovascular diseases, and statins are used extensively in the clinic to prevent progression of atherosclerosis. Myopathy is an adverse effect of all statins, but the most severe form of myotoxicity, rhabdomyolysis, is rare with currently used statins (Bays, 2006; Cziraky et al., 2006; Graham et al., 2004). High statin doses, as well as certain drug-drug interactions, particularly those leading to high statin concentrations in peripheral blood and muscle cells, increase the risk of myotoxicity (Abdul-Ghaffar and el-Sonbaty, 1995; Chang et al., 2004; Knoll et al., 1993; Maxa et al., 2002; Pierce et al., 1990; Pogson et al., 1999; Tal et al., 1997).

Because of their extensive clinical use, the likelihood that new drugs would be co-administered with statins is high. Therefore, the drug-drug interaction potential with statins is of great importance for the clinical safety of new drug candidates.

The statins enter the hepatocytes by both passive and active transport (Shitara and Sugiyama, 2006). The extend of passive uptake is varying according to the lipophilicity of the statin (Shitara and Sugiyama, 2006). The active uptake into hepatocytes are mediated primarily by the OATP1B1 transporter (Shitara and Sugiyama, 2006). Atorvastatin, pravastatin, cerivastatin, pitavastatin and rosuvastatin are all reported to be substrates of OATP1B1, with pravastatin and atorvastatin as the most extensively studied agents (Fujino et al., 2004; Hsiang et al., 1999; Kameyama et al., 2005; Lau et al., 2006; Nakai et al., 2001; Schneck et al., 2004; Shitara et al., 2003a).

Most statins are administered as the orally active β -hydroxy acid form, except from lovastatin and simvastatin (Shitara and Sugiyama, 2006). Observation of both acid and lactone forms in the systemic circulation after administration of atorvastatin, lovasatatin, simvastatin and cerivastatin indicates an interconversion between the acid and lactone forms of these statins (Kantola et al., 1998a; Kantola et al., 1998b; Neuvonen and Jalava, 1996; Prueksaritanont et al., 2002). Chen et al examined the interaction of statins (pravastatin, atorvastatin acid an lactone, simvastatin acid and lactone, lovastatin acid and lactone) with P-gp, MRP2 and OATP1B1, and observed that the the IC_{50} values for the P-gp and MRP2 for all statins in acid form were up to 10-fold lower than for the corresponding lactone (Chen et al., 2005). In contrast, inhibition of OATP1B1 by these statins showed that the acid form was more potent than the lactone form, with an IC_{50} value 3- to 7-fold lower for the acid form (Chen et al., 2005).

1.3.1 Pravastatin

Pravastatin is administered as the open acid form (Figure 1.5). Pravastatin has a high affinity for HMG-CoA reductase with inhibition constant (K_i) of 44.1 nM (McTaggart et al., 2001). The $\log D$ value (pH 7.0) of pravastatin is -0.47 (Ishigami et al., 2001), indicating limited membrane permeability and low passive diffusion. Pravastatin is actively transported from the portal blood into hepatocytes by OATP1B1 (Hsiang et al., 1999; Nakai et al., 2001). Pravastatin is not significantly metabolized by the cytochrome P-450 enzymes (Hatanaka, 2000), and biliary excretion is a major route of elimination. The excretion into the bile is mediated by several efflux transporters; MRP2, P-gp, BCRP and BSEP (Figure 1.3) (Hirano et al., 2005; Matsushima et al., 2005; Sasaki et al., 2002). MRP2 has the highest transport activity (Matsushima et al., 2005).

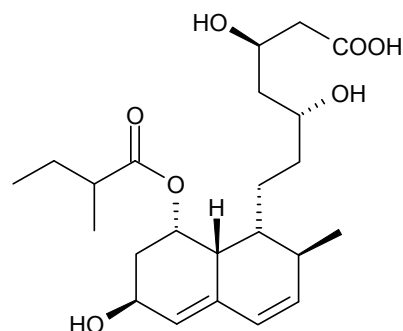


Figure 1.5 Chemical structure of the open acid form of pravastatin.

Expression and function of OATP1B1 is considered the rate-limiting step in the hepatic clearance of pravastatin (Yamazaki et al., 1996). Altered systemic exposure of pravastatin as a result of transporter-mediated drug-drug interactions or *SLCO1B1* polymorphisms could therefore change the clinical response. Although pravastatin is not involved in P450-mediated drug-drug interactions, it is likely to be affected by transporter-mediated drug-drug interactions when co-administration with inhibitors of OATP1B1 (Kyrklund et al., 2003; Nakagomi-Hagihara et al., 2007; Seithel et al., 2007; Yamazaki et al., 2005). Nakagomi-Hagihara et al. showed that when pravastatin was co-administrated with the OATP1B1 inhibitor gemfibrozil, the AUC of pravastatin increased approximately 2-fold (Nakagomi-Hagihara et al., 2007). The same results were reported by Kyrklund et al. (Kyrklund et al., 2003).

Effects of the *SLCO1B1* polymorphisms on the transport activity *in vitro* and on the pharmacokinetics in human have been investigated in recent studies. The *SLCO1B1* *5, *15 and *17 haplotypes are associated with increased plasma concentration of pravastatin (Mwinyi et al., 2004; Niemi et al., 2005; Niemi et al., 2004; Nishizato et al., 2003). Niemi et al. showed that AUC of pravastatin increased with 93% and 130% in heterozygote carriers of *15 and *17, respectively, compared to subjects with reference haplotype (Niemi et al., 2004). In addition, 521T>C polymorphism is associated with reduced total cholesterol-lowering effect of pravastatin (Niemi et al., 2005; Tachibana-limori et al., 2004; Zhang et al., 2006). Zhang et al. showed an attenuated total cholesterol-lowering effect in patients with 521TC heterozygote genotype (-14.5% reduction), compared to 521TT homocoygote genotype (-22.4% reduction) (Zhang et al., 2006). On the contrary, the *SLCO1B1* *1b haplotype, is associated with decreased plasma concentration of pravastatin (Maeda et al., 2006; Mwinyi et al., 2004). Mwinyi et al. reported that AUC of pravastatin was 35% lower in subjects carrying the *1b haplotype than in the subjects with *1a/*1a reference genotype (Mwinyi et al., 2004).

The myotoxic effects of statins are concentration-dependent (Thompson et al., 2003), and subjects with increased plasma concentration of pravastatin due to transporter-mediated drug-drug interactions or certain polymorphisms in the gene encoding OATP1B1, are more susceptible to pravastatin-induced myopathy (Ballantyne et al., 2003; Biggs et al., 2006; Chang et al., 2004; Graham et al., 2004; Omar et al., 2001; Regazzi et al., 1993; Schindler et

al., 2007). Morimoto et al. found that the frequency of *SLCO1B1* *15 is significantly higher in patients who experienced myopathy after receiving pravastatin or atorvastatin than in patients without myopathy (Morimoto et al., 2004).

1.3.2 Atorvastatin

Atorvastatin is administered as the open acid form (Figure 1.6). Atorvastatin has higher affinity for HMG-CoA reductase than pravastatin with an inhibition constant (K_i) of 8.2 nM (McTaggart et al., 2001). The $\log D$ value (pH 7.0) of atorvastatin is 1.53 (Ishigami et al., 2001), indicating that atorvastatin undergoes passive diffusion to a greater extent than pravastatin. Atorvastatin is also a substrate of OATP1B1 and enters the hepatocytes via carrier-mediated uptake (Chen et al., 2005; Kameyama et al., 2005; Lau et al., 2007; Lau et al., 2006). In hepatocytes atorvastatin are predominantly metabolized by cytochrome P450 3A4 (CYP3A4) (Lennernas, 2003). Atorvastatin is also excreted into bile by P-gp and MRP2 (Chen et al., 2005; Lau et al., 2006).

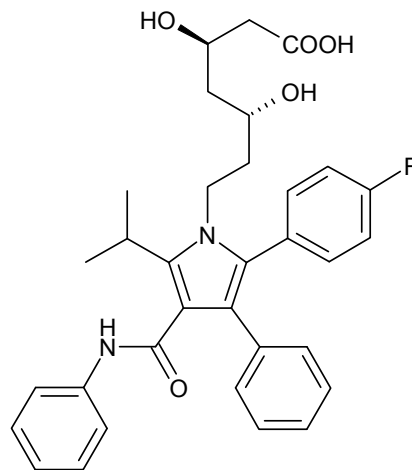


Figure 1.6 Chemical structure of the open acid form of atorvastatin.

The clearance of atorvastatin is affected by both the metabolic rate and the uptake rate (Shitara and Sugiyama, 2006), which implies susceptibility to CYP3A4- as well as OATP1B1-mediated drug-drug interactions (Lau et al., 2007; Lau et al., 2006; Lau et al., 2004; Lennernas, 2003; Åsberg et al., 2001). Lau et al. reported that co-administration with rifampicin acutely increased the AUC of atorvastatin around 6-fold (Lau et al., 2007). This was explained as an inhibitor effect of the OATP1B1 transporter. Hermann et al. showed a 10-fold increase in AUC of atorvastatin in patients treated with ciclosporine (Hermann et al., 2004), possibly due to inhibition of OATP1B1.

Like pravastatin, *SLCO1B1* polymorphisms can cause interindividual differences in plasma concentrations of atorvastatin (Kameyama et al., 2005; Pasanen et al., 2007). Pasanen et al. reported that subjects with the *SLCO1B1* 521CC genotype had a 144% or 61% higher AUC of atorvastatin than those with the 521TT or 521TC genotype, respectively (Pasanen et al., 2007).

The myotoxic effects of statins are concentration-dependent (Thompson et al., 2003), and subjects with increased plasma concentration of atorvastatin due to drug-drug interactions or certain polymorphisms in the gene encoding OATP1B1, are more susceptible to atorvastatin-induced myopathy (Ballantyne et al., 2003; Graham et al., 2004; Omar et al., 2001). As mentioned in section 1.3.1, Morimoto et al. found that the frequency of *SLCO1B1* *15 is significantly higher in patients who experienced myopathy after receiving pravastatin or atorvastatin than in patients without myopathy (Morimoto et al., 2004). On the contrary, Hermann et al. reported no differences in frequencies of *SLCO1B1*, *MDR1*, and *CYP3A5* polymorphisms between patients with atorvastatin-related myopathy and the control group (Hermann et al., 2006). This study also showed that the exposure of atorvastatin was unchanged, but the lactone and acid metabolites were increased several-fold in patients with atorvastatin-induced myopathy.

1.4 *In vitro* transport systems

For the pharmaceutical industry it is of importance to develop *in vitro* transport models with the ability to predict possible genetic variability and drug-drug interactions of a new compound. This is valuable information in an early stage of drug development when determining whether a compound should be included in further trial, and if so, the clinical pharmacokinetic studies that should be performed. *In vitro* transport models are also important tools when determining pharmacokinetic characteristics of existing, uncharacterized drugs.

A variety of different model systems have been applied to characterize the mechanisms of drug transport and estimate the elimination rates of drugs via liver. Isolated hepatocytes are often used as model system, and recent progress in cryopreservation techniques have enabled preservation of frozen human hepatocytes in a way that most of their transporter activity is retained (Shitara et al., 2003b). Membrane vesicles prepared from the sinusoidal and bile canalicular membrane in the liver are readily available for the study of hepatobiliary transport, but a possible limitation of the model system is the requirement of a driving force for transport (i.e. ATP hydrolysis) (Shitara et al., 2005). Transfected cell systems expressing a specific transporter are used to obtain the kinetic parameters for the target transporter. cDNA transfected cells or cRNA injected oocytes can be used as gene expression systems. More recently, cultured cells stably transfected with both uptake and efflux transporters have become available. In these systems, transcellular transport of a compound can be measured. As human tissue samples are scarcely distributed, the transporter-expressing systems are valuable tools in drug transport studies (Shitara et al., 2005).

1.4.1 HEK293 cells

Human embryonic kidney (HEK) cells are extensively used as an expression tool for recombinant proteins (Thomas and Smart, 2005). For transport studies, HEK293 cells are transfected with a gene encoding a transport protein of interest. The result of the transfection is a HEK293 cell line overexpressing the specific transport protein. Transfected HEK293 cells are widely used because of its easy reproduction and maintenance, ability of transfection using a wide variety of methods, high efficiency of transfection and protein production, and reliable translation and processing of proteins (Thomas and Smart, 2005). HEK293 cells grow in epithelial-like monolayers and have become increasingly recognized as models for transporter studies. HEK293 cells transfected with a plasmid containing the *SLCO1B1* gene is a cell line expressing the transport protein OATP1B1. These cells are simple cell systems overexpressing OATP1B1. HEK293 cells transfected with the empty vector pT-REX can be used as control cells in transport studies with HEK293/OATP1B1 cells.

1.4.2 *Xenopus laevis* oocytes

Xenopus laevis oocytes are oocytes obtained from a frog in the genus *Xenopus*. The ease of manipulations in the embryos has given them an important place in developmental biology. cRNA encoding the protein of interest is injected into *Xenopus laevis* oocytes, leading to the expression of the specific transporter. *Xenopus laevis* oocytes injected with cRNA encoding OATP1B1 is a simple transport system overexpressing OATP1B1. Water injected *Xenopus laevis* oocytes can be used as control system in transport studies with OATP1B1 cRNA injected oocytes.

1.4.3 HepaRG cells

HepaRG cells are cells derived from a human hepatocellular carcinoma (Le Vee et al., 2006). This is a cell system expressing naturally occurring levels of a mixture of transporters and enzymes. HepaRG cells have the unique properties of maintaining significant levels of hepatocytes functions, including enzyme and transporter activity (Aninat et al., 2006; Le Vee et al., 2006). HepaRG cells can be grown in monolayers, which make them suitable for uptake studies. Compared to the transport models described above (1.4.1, 1.4.2), this is a complex cell system with retained transporter and enzyme multiplicity.

1.5 Transport kinetics

Drugs cross membranes either by passive or active, carrier-mediated processes. The total transport of a drug into the cell, U_{total} , can be expressed as:

$$U_{total} = U_{active} + U_{passive} \quad (\text{Equation 1.1})$$

, where U_{active} is the active uptake of the drug mediated by carriers, and $U_{passive}$ is the passive diffusion of the drug across the membrane.

Active uptake transport is similar to enzyme-catalyzed reactions, and the Michaelis-Menten model can be used to determine uptake kinetics of drug transport through membrane drug transporters. The relationship between transport protein and substrate can be expressed as:



, where T is the transport protein, TS is the complex of transport protein and substrate, S₁ and S₂ are the substrates on side 1 respectively side 2 of the membrane. The initial velocity (V_{0_total}) of a transport process at steady state, including active and passive transport, at a given substrate concentration (S), is given by the modified Michaelis-Menten equation:

$$V_{0_total} = \frac{V_{max}[S]}{K_m[S]} + P[S] \quad (\text{Equation 1.2})$$

, where V_{max} is the maximum velocity of the transport process under given conditions, K_m is the Michaelis constant, and P is the constant describing passive diffusion. The initial velocity of the passive diffusion, V_{0_passive}, at a given substrate concentration (S), is expressed as:

$$V_{0_passive} = P \times [S] \quad (\text{Equation 1.3})$$

, where P is the constant describing passive diffusion. Equation 1.1-1.3 gives an expression of the initial uptake rate of the carrier-mediated uptake, V_{0_active}, at a given substrate concentration (S):

$$V_{0_active} = \frac{V_{max}[S]}{K_m[S]} \quad (\text{Equation 1.4})$$

, where V_{max} is the maximum velocity of the transport process under given conditions and K_m is the Michaelis constant. This is the Michealis-Menten equation. Equation 1.2, 1.3 and 1.4 are illustrated in Figure 1.7 for compounds exhibiting low and high passive diffusion. Equation 1.2, 1.3 and 1.4 are illustrated as the total, passive and active uptake, respectively.

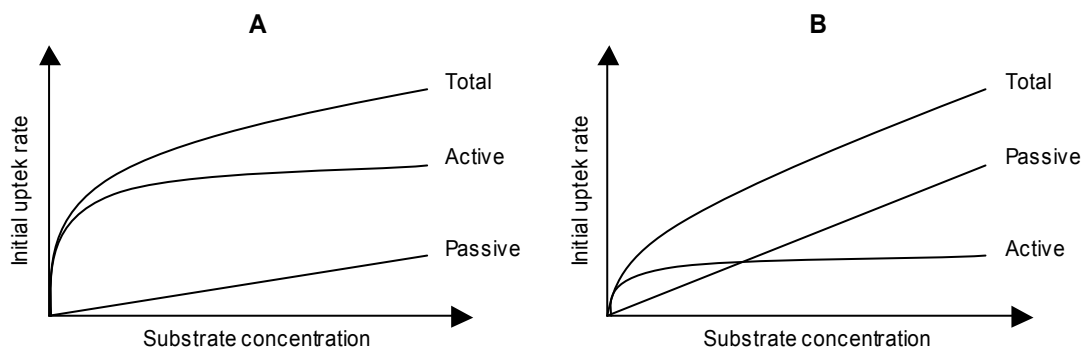


Figure 1.7 Total, passive and active uptake of a drug exhibiting low passive diffusion (A) and high passive diffusion (B).

The Michaelis constant, K_m, is defined as the [S] at ½ V_{max} (Figure 1.8). K_m is an expression of the substrate affinity for the transporter. A low K_m corresponds to a high affinity. V_{max} is an expression of the capacity of the process.

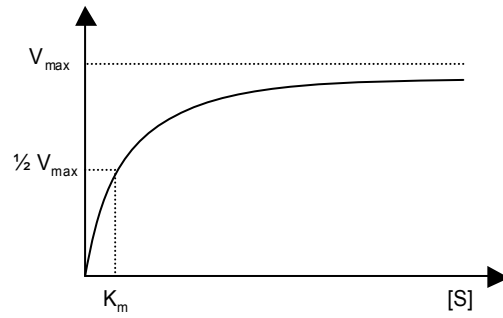


Figure 1.8 The uptake kinetics of an actively transported compound following the Michaelis-Menten kinetics. K_m represents the Michaelis constant, the substrate concentration at which the initial uptake rate is half maximal.

The initial velocity/uptake rate is given by:

$$V_0 = \frac{U_2 - U_1}{t_2 - t_1} \quad (\text{Equation 1.5})$$

, where t_1 and t_2 are two early points of time within the linear interval of uptake, and U_1 and U_2 are uptake at t_1 and t_2 respectively.

To apply the Michaelis-Menten equation (Equation 1.4), the time point chosen has to be within the linear interval of uptake. A low and high concentration is chosen, and uptake is measured against time. According to these results, a point of time is chosen where the initial uptake rate at both concentrations is within the linear interval. This time of incubation is applied in the further concentration dependence uptake studies.

Co-incubation of inhibitor and substrate of a certain membrane transporter changes the uptake kinetics of the substrate. The presence of a constant concentration of a *competitive inhibitor* affects the affinity by increasing K_m , while V_{max} remains constant. *Uncompetitive inhibitors* affect the uptake kinetics by decreasing both V_{max} and K_m . *Non-competitive inhibitors* decrease the capacity of the process (V_{max}), while K_m is not affected.

1.6 Purpose of the study

The purpose of the present study is to evaluate and compare three existing *in vitro* models expressing the membrane drug transporter OATP1B1. Two of the models are simple systems overexpressing OATP1B1, while the third one is a human cell line expressing natural levels of OATP1B1, in addition to other transport proteins and enzymes found in human hepatocytes. Uptake studies of three known substrates for OATP1B1, estradiol-17 β -D-glucuronide, atorvastatin and pravastatin, will be applied to compare the systems.

2 MATERIALS AND METHODS

2.1 Materials

³H-estradiol-17 β -D-glucuronide (53 Ci/mmol, 46.9 Ci/mmol) was purchased from PerkinElmer (Boston, MA, USA). ³H-atorvastatin (5 Ci/mmol) was purchased from American Radiolabeled Chemicals Inc. (St Louis, MO, USA). ³H-pravastatin (20 Ci/mmol) was purchased from Moravек Biochemicals (Brea, CA, USA). Atorvastatin calcium and pravastatin sodium were purchased from Toronto Research Chemical Inc. (Toronto, Canada). Dimethylsulfoxide (DMSO) and estradiol-17 β -D-glucuronide were purchased from Sigma-Aldrich (Steinheim, Germany). D-MEM/F-12 (1:1) (1x) liquid with GlutaMAXTM I, D-PBS without CaCl₂ and MgCl₂ (D-PBS⁻), foetal calf serum (FCS), geneticin (G418, 50 mg/ml), Hanks balanced salt solution (HBSS) with CaCl₂ and MgCl₂, HEPES (1 M), L-glutamine (200 mM), PEST (Penicillin (100 U/ml)-Streptomycin (100 μ g/ml)-solution), and Trypsin-EDTA (1x) 0.05 % with EDTA 4Na, were purchased from Gibco/Invitrogen (Paisley, UK). DHI Medium was purchased from SAFC Biosciences (Andover, UK). Sodium butyrate was purchased from Merck (Schuchardt, Germany). HepaRG medium containing DMSO and basal HepaRG medium were purchased from Biopredic International (Rennes, France). Sodium transport buffer, ND96 buffer and 10% SDS buffer were purchased from BD Biosciences (Woburn, MA, USA). SuperScript III First-Strand Synthesis System for RT-PCR and Trizol reagent were acquired from Invitrogen (Stockholm, Sweden). The primers and probe used in this study were provided by Applied Biosystems (Cheshire, UK). Taqman Assay on Demand and Taqman[®] Universal Master Mix were purchased from Applied Biosystems (Stockholm, Sweden). All other chemicals were of analytical grade and highest quality available.

2.2 Cell culturing and seeding

2.2.1 HEK 293 cells

HEK293 cells stably transfected with human OATP1B1 and HEK293 cells stably transfected with empty vector (pT-REX) were obtained from the GADGET project at AstraZeneca Södertälje/Lund.

The culture medium was composed of 500 ml DHI Medium, 58 ml heat-inactivated FCS (Foetal Calf Serum), 6 ml 200 mM L-glutamine, 6 ml 180 mM sterile stock solution of CaCl₂ and 6 ml 50 mg/ml stock solution of geneticin. The HEK293 cells were grown in 75cm² plastic culture flasks NunClonTM Surface (NuncTM, Roskilde, Denmark) at 37°C in a humid atmosphere (5% CO₂), CO₂ incubator (LabRum Klimat AB, Stockholm Sweden). The culture medium was changed every 2-3 days.

The cells were split into a new passage approximately twice a week at 70-80% confluence. Old medium was removed by aspiration, and the cells were washed with 5 ml D-PBS⁻. 2 ml trypsin/EDTA (0.05%) was added. The flask was gently shaken after approximately 1 minute to detach the cells, and the cells were collected in a centrifuge tube containing 10 ml pre-heated (37°C) culture medium. The tube was centrifuged 4 minutes at 800 rpm (Centrifuge Rotina 24TM, Hettich, Germany). The supernatant was removed from the cells, and the pellet was resuspended in 20 ml pre-heated medium. The cells were counted in the NucleoCounter[®] (ChemoMetec A/S, Denmark). Approximately 3 million cells were seeded into new 75 cm² flasks containing 10 ml culture medium, and grown for approximately 4 days before new splitting or seeding on plates.

For uptake studies, the HEK293 cells were seeded in poly-D-lysine coated 24-well cell culture plates at 0.3 million cells per well (BD BioCoatTM Multiwell Cell Culture Plates, BD Bioscience), and incubated for 72 hours before experimentation.

The conditions described above were chosen after initial testing of conditions in uptake studies performed on estradiol-17 β -D-glucuronide, the model substrate for OATP1B1. This was performed due to deviations from previously reported K_m values of estradiol-17 β -D-glucuronide (Iwai et al., 2004; Konig et al., 2000) in preliminary experiments. The following cell culturing conditions were tested and evaluated;

- Another culture medium consisting of 500 ml D-MEM/F-12 (1:1) (1x) liquid with GlutaMAXTM I, 50 ml heat-inactivated FCS, 2.5 ml PEST and 5 ml Geneticin (50 mg/ml) was used.
- 1 million HEK293 cells were seeded into 75 cm² flasks with 25 ml of the culture medium above, and grown for 7 days before sub cultivation.
- The cells were not trypsinated during sub cultivation.
- The experiments were performed at a different laboratory (AstraZeneca R&D Mölndal and AstraZeneca R&D Lund).
- Experiments were performed on HEK293 cells stored at AstraZeneca R&D Lund. The transfected HEK293 cells used in the other experiments had been seeded, sub cultivated and stored at AstraZeneca Alderley Park before they were shipped to AstraZeneca R&D Mölndal.
- Another amount of cells, 0.5 million cells/well, were seeded in the 24-well plates for the uptake studies.
- The cells seeded in 24-well plates were treated with sodium butyrate. The culture medium was changed to medium containing 10 μ M Na-butyrate 24 hours prior to experimentation. Sodium butyrate treatment is supposed to increase the expression of proteins (in this case the expression of OATP1B1) (Kruh, 1982).

It should be noted that the time dependence uptake studies with estradiol-17 β -D-glucuronide (Figure 3.1 and 3.2) were performed before the conditions were optimized. Results from these uptake studies were satisfying (high uptake ratio), and did not indicate the need of condition improvements.

2.2.2 HepaRG cells

The differentiated HepaRG cells (passages 18 and 19) were purchased from Biopredic International (Rennes, France). The experiments were performed with 24-well plates (50 000 cells seeded per well). The cells were initially grown in William's medium E with glutamax-I supplemented with 10 % FBS, 100 IU/ml penicillin, 100 μ g/ml streptomycin, 5 μ g/ml bovine insulin and 50 μ M hydrocortisone hemisuccinate. At confluence, 2% DMSO was added to the medium in order to differentiate the cells into hepatocyte-like morphology. The cells were cultured in differentiation medium for 3 weeks before shipment to AstraZeneca R&D Mölndal.

At arrival the DMSO-containing HepaRG medium was renewed. The old medium was removed by aspiration and 400 μ l DMSO-containing HepaRG medium was added to each well. The cells were given 24 hours to recover. After 24 to 48 hours the medium was changed to basal HepaRG medium (William's medium E with glutamax-I supplemented with 100 IU/ml penicillin, 100 μ g/ml streptomycin, 4 μ g/ml bovine insulin and 50 μ M hydrocortisone hemisuccinate). The cells were cultured in basal HepaRG medium for 24 hours before the experiment was started.

2.3 Preperation of *Xenopus laevis* oocytes

Xenopus laevis oocytes microinjected with OATP1B1 cRNA and water-injected controls were purchased from BD Gentest Discovery Labware Inc. (BD Biosciences, Woburn, MA, USA). Before shipping to AstraZeneca R&D Mölndal, the oocytes were prepared the following way. OATP1B1 was cloned from human liver by PCR using gene-specific primers, and cDNA was isolated. To obtain higher expression and function of the human transporter in the oocyte, an oocyte expression vector was engineered by inserting *Xenopus* β -globin 5' and 3' untranslated region into pBluescript II KS (+) (Stratagene). cDNAs of OATP1B1 were subcloned into the vector with the 5' and 3' untranslated regions of the *Xenopus* β -globin gene flanking the insert. cRNAs were synthesized by using T3 polymerase (Stratagene). Oocytes were harvested and digested with collagenase D (Boehringer Mannheim). Fifty nanoliters of cRNA (~ 0.4 ng/nl) or water was injected individually into defolliculated oocytes. Oocytes were immediately transported to AstraZeneca R&D Mölndal. The temperature was kept between 14°C and 20°C.

The oocytes were delivered in BD Falcon™ 12-well plates, diluted in ND96 Buffer. Upon arrival the oocytes were inspected under microscope (Olympus CK2, Olympus America Inc.,

NY, USA) to confirm viability. Dead, dying or broken oocytes were removed by a pipette, and the ND96 Buffer was replaced. The oocytes were stored at 14°C to 20°C. Uptake experiments were performed within 4 days after injection.

2.4 Transport experiments with HEK293 cells and HepaRG cells

2.4.1 Preparation of buffer solution and test solutions

The buffer used in the transport experiments consisted of HBSS buffered with 25 mM HEPES to pH 7.4. Radiolabeled compounds were used to study the transport. The radiolabeled compounds were diluted directly in pre-heated buffer solution to obtain the required concentrations, while non-labeled compounds were dissolved in DMSO before dilution in pre-heated buffer solution. In the concentration dependence uptake studies, each solution in the dilution series contained the same amount of radiolabeled compound. Experiments were performed with estradiol-17 β -D-glucuronide on HEK293 cells to evaluate whether dilution of both radiolabeled and non-labeled compound gave a different K_m value.

2.4.2 Uptake experiments with HEK293 cells

Prior to the experiments, cell confluence was examined visually under the microscope (Olympus CK2, Olympus America Inc., NY, USA) to assess equal growth in all cultures and wells. Culture medium was removed from the wells by aspiration, and the HEK293 cells were washed twice with 700 μ l/well pre-heated (37°C) buffer solution. 250 μ l pre-heated buffer were added to each well, and the cells were incubated for 10 minutes in a shake incubator (THERMOstar, BMG LabVision, Stockholm) set to a temperature of 37°C and 0 rpm. The experiment was started by adding 250 μ l/well pre-heated test solution. During the experiment, the plate incubator was set to a temperature of 37°C and 450 rpm. The experiments were stopped at a given time by discarding the plate. The cells were immediately washed three times with 1000 μ l/well ice cold (4°C) buffer, and lysed by adding 500 μ l 0.2 M NaOH to each well. The plates were placed in the fridge (4°C) for approximately one hour.

The experiments were performed on HEK293 cells transfected with human OATP1B1 and control cells (HEK293 cells transfected with the empty vector pT-REX). Active uptake was either expressed as the difference or ratio between uptake into HEK293/OATP1B1 and HEK293/pT-REX cells. A difference >0 or ratio >1 was interpreted as active, OATP-mediated uptake.

Uptake studies were performed with three different substances; estradiol-17 β -D-glucuronide, atorvastatin and pravastatin. *Time dependent uptake* was determined by measuring uptake of substance at six different time points over 10-15 minutes at one or two given concentrations. The approximate linear interval of uptake for each substance was determined by visual

expedition. *Concentration dependent uptake* was determined by measuring uptake at eight different concentrations at a time point within the linear interval of uptake. The concentrations chosen were depending on the substrate used in the experiment.

The linear interval of the time dependent uptake should be determined at a low and a high substance concentration to assure that the uptake is linear in the whole range of concentrations applied in the concentration dependence uptake study. The reasons why the uptake studies on HEK293 cells with atorvastatin and pravastatin were performed only at low concentrations, were time deficiency, the high costs of these substances, and to determine whether this low concentration of radiolabeled substance gave an uptake detectable in the liquid scintillation counter.

2.4.3 Uptake experiments with HepaRG cells

Prior to the experiments cell confluence was examined visually under the microscope (Olympus CK2, Olympus America Inc., NY, USA) to assess equal growth in all wells.

Uptake assay at 37°C

Culture medium was removed from the wells by aspiration, and the HepaRG cells were washed twice with 700 µl/well pre-heated (37°C) buffer solution. 250 µl pre-heated buffer was added to each well, and the cells were incubated for 10 minutes in a shake incubator (THERMOstar, BMG LabVision, Stockholm) set to a temperature of 37°C and 0 rpm. The experiment was started by adding 250 µl/well pre-heated test solution. During the experiment, the plate incubator was set to a temperature of 37°C and 0 rpm. The experiments were stopped at a given time by discarding the plate. The cells were immediately washed three times with 1000 µl/well ice cold (4°C) buffer, and lysed by adding 500 µl 0.2 M NaOH to each well. The plates were placed in the fridge (4°C) for approximately one hour.

Uptake assay at 4°C

The 24-well plate was placed on ice. Culture medium was removed from the wells by aspiration, and the HepaRG cells were washed twice with 700 µl/well ice cold (4°C) buffer solution. 250 µl ice cold buffer was added to each well, and the cells were incubated for 10 min. The experiment was started by adding 250 µl/well ice cold test solution. The experiments were stopped at a given time by discarding the plate. The cells were immediately washed three times with 1000 µl/well ice cold buffer, and lysed by adding 500 µl 0.2 M NaOH to each well. The plates were placed in the fridge (4°C) for approximately one hour.

The experiments were performed on HepaRG cells at two different temperatures (37°C and 4°C). HepaRG cells are human cells expressing a natural level of transporters, including OATP1B1. There exist no control cells. To determine the passive uptake into HepaRG cells, the experiments were performed at 4°C. At this temperature the transporters are out of

function. Active uptake was either expressed as the difference or ratio between uptake into HepaRG cells at 37°C and 4°C. A difference >0 or ratio >1 was interpreted as active, OATP-mediated uptake.

Uptake studies were performed with three different substances; estradiol-17 β -D-glucuronide, atorvastatin and pravastatin. *Time dependent uptake* was determined by measuring uptake of substance at six different time points over 10 minutes at a given concentration. The approximate linear interval of uptake for each substance was determined by visual expedition. *Concentration dependent uptake* was determined by measuring uptake at eight different concentrations at a time point within the linear interval of uptake. The concentrations chosen were depending on the substrate used in the experiment.

The linear interval of the time dependent uptake should be determined at a low and a high substance concentration to assure that the uptake is linear in the whole range of concentrations applied in the concentration dependence uptake study. The reasons why the uptake studies on HepaRG cells with atorvastatin and pravastatin were performed only at low concentrations and with one replicate, were the very high costs of the HepaRG cells and of these substances, and to determine whether the low concentration of radiolabeled substance gave an uptake detectable in the liquid scintillation counter.

2.5 Transport experiments with *Xenopus laevis* oocytes

2.5.1 Preparation of buffer solution and test solutions

Sodium transport buffer from BD Biosciences was used in the first experiments with the oocytes. In the later experiments, transport buffer prepared at the laboratory was used. The buffer contained 10 mM 2-[4-(2-hydroxyethyl)-1-piperazinyl]ethanesulfonic acid/Tris, 100 mM NaCl, 1 mM MgCl₂, 2 mM KCl, and 1 mM CaCl₂, adjusted to pH 7.4. Radiolabeled compounds were used to study the transport. The radiolabeled compounds were diluted in pre-heated buffer solution to a concentration of 1 μ M. Non-labeled compounds were dissolved in DMSO and then diluted in pre-heated buffer solution to obtain the required test concentrations.

2.5.2 Uptake experiments with oocytes

Upon experiments, the oocytes were inspected visually under microscope (Olympus CK2, Olympus America Inc., NY, USA) to confirm viability. Dead, dying or broken oocytes were removed by a pipette. Depending on the study (time dependence or concentration dependence), a specific number of oocytes were placed in a test tube made of glass. The ND96 Buffer was removed by aspiration, and the oocytes were washed three times with 3 ml of room temperature sodium buffer. 100 μ l test solution was added after removing the sodium

buffer for the third time. The experiment was stopped at a given time by removing the test solution by aspiration. The oocytes were immediately washed three times with 3 ml ice cold (4°C) sodium buffer. A final aliquot of 3 ml ice cold buffer was added.

The experiments were performed on oocytes injected with OATP1B1 cRNA and oocytes injected with water. The uptake into water injected oocytes is an expression of the passive uptake of substance into *Xenopus laevis* oocytes. Active uptake was either expressed as the difference or ratio between uptake into OATP1B1 cRNA injected and water injected oocytes. A difference >0 or ratio >1 was interpreted as active, OATP-mediated uptake.

Uptake studies were performed with three different substances; estradiol-17 β -D-glucuronide, atorvastatin and pravastatin. *Time dependent uptake* was determined by measuring uptake into three oocytes at four different time points over 20-90 minutes at a given concentration. The approximate linear interval of uptake for each substance was determined by visual expedition. *Concentration dependent uptake* was determined by measuring uptake into eight oocytes at eight different concentrations at a time point within the linear interval of uptake. The concentrations chosen were depending on the substrate used in the experiment.

The linear interval of the time dependent uptake should be determined at a low and a high substance concentration to assure that the uptake is linear in the whole range of concentrations applied in the concentration dependence uptake study. The reason why the uptake studies on the oocytes were performed only at one substance concentration was the high costs of the oocytes.

2.6 Analysis

2.6.1 Liquid scintillation counting

HEK293 cells and HepaRG cells. The 24-well plate was shaken in a plate shaker for 1 min at high speed. 300 μ l cell lysate was transferred to a scintillation vial, and the sample was neutralized by adding 150 μ l 0.2 M HCl. 10 ml scintillation liquid (OptiPhase HiSafe 2, Fisher Chemicals, UK) was added to each vial, and the sample was mixed (Vortex). The radioactivity was measured in a Wallac LS-counter (Wallac Win Spectral, 1414 Liquid Scintillation Counter, PerkinElmer).

Oocytes. The oocytes were transferred to scintillation vials (one oocyte per vial). A drop of buffer from the last wash was placed in a separate scintillation vial to act as a negative control. The oocytes were lysed by adding 150 μ l of 10% SDS buffer to each scintillation vial, and incubated on an orbital shaker for 10 minutes at room temperature. 5 ml scintillation liquid (OptiPhase HiSafe 2, Fisher Chemicals, UK) was added to each vial, and the sample was

mixed (Vortex). The radioactivity was measured in a Wallac LS-counter (Wallac Win Spectral, 1414 Liquid Scintillation Counter, PerkinElmer).

Uptake of radiolabeled compound was measured by the number of disintegrations per minute (dpm). In the time dependence uptake studies, the obtained data was converted into pmol/mg protein according to the following equation:

$$pmol / mg _ protein = \frac{dpm \times 10^{12} _ pmol / mol}{2.22 \cdot 10^{12} _ dpm / Ci \times spec _ activity(Ci / mol)} \quad (Equation \ 2.1)$$

, where dpm is disintegrations per minute for the uptake sample, spec activity is the specific activity of the radiolabeled compound, and mg protein is the amount of protein per well in mg.

In the experiments where both cold and warm compound were used, the total uptake was calculated by the following equation:

$$pmol / mg _ protein = \frac{dpm \times ratio _ cold / warm \times 10^{12} _ pmol / mol}{2.22 \cdot 10^{12} _ dpm / Ci \times spec _ activity(Ci / mol)} \quad (Equation \ 2.2)$$

, where dpm is disintegrations per minute for the uptake sample, ratio cold/warm is the ratio between radioactive unlabeled and labeled compound, spec activity is the specific activity of the radiolabeled compound, and mg protein is the amount of protein per well in mg.

2.6.2 Protein quantification

Protein content in HEK293 cells and HepaRG cells were quantified using the method of Markwell (Markwell et al., 1978), which is a modified method of the Lowry procedure (Lowry et al., 1951). 75 µl aliquots of cell lysate were neutralized with 75 µl 0.2 M HCl. These samples were diluted 10x and 20x in water. The proteins were prepared by mixing 100 µl aliquots of lysate solution with 300 µl of Reagent solution 1 ([4% Na₂CO₃, 0.2M NaOH, 0.32% K-Na-tartrate], 2 % SDS and 4% CuSO₄·5H₂O in the proportion 75:75:1.5). After incubation for approximately 30 minutes, the samples were mixed with 30 µl of Reagent solution 2 (Folin-Ciocalteu phenol reagent and ELGA water in the proportion 1:1), and incubated for 45 minutes. The absorbance was measured at a wavelength of 660 nm, and protein content quantified in a multi-detection microplate reader, SpectraMax[®] M5 (Molecular Devices, Sunnyvale, CA, USA). The results were processed with the software program SOFTMax Pro v4.8 using BSA as calibration standard.

2.6.3 mRNA quantification

The amount of OATP1B1 mRNA in HEK293/OATP1B1 and HEK293/pT-REX cells was determined to compare the expression of OATP1B1 in the two cell lines. mRNA quantification

of hOATP1B1 in HEK293/OATP1B1 cells after treatment with sodium butyrate was also determined.

RNA extraction. 500 μ l Trizol was added to each well (24-well plate) to lysate the cells, and total RNA from HEK293 cells was prepared according to manufacturers' instructions (Invitrogen). RNA quantity was determined spectrophotometrically using a GenQuant pro RNA/DNA calculator (Biochrom, Cambridge, UK). cDNA was prepared from 0.5 μ g of total RNA using the SuperScript™ III First-Strand Synthesis System for RT-PCR with random hexamer primers according to the manufacturer's protocol (Invitrogen).

Real-Time PCR. Real-time PCR for human OATP1B1 mRNA levels was performed by a 7500 Sequence Detector (Applied Biosystems, Foster City, CA, USA) and manufacturer designed Assay on Demand for OATP1B1, MVP and PPIA. MVP and PPIA were used as endogenous control genes. Briefly described, the reaction mixture (25 μ l per well) contained 30 ng cDNA, 12.5 μ l 2xTaqman Universal Master Mix, 1.25 μ l Assay on Demand and 6.2 μ l RNase free water. The thermal cycle had initial steps of 50°C for 2 min and a 10 min step at 95°C followed by 40 PCR cycles of 95°C for 15 s, and finally 60°C for 1 min. Each sample was analyzed in triplicate and data was analyzed using the 7500 Sequence detector software v1.3.1 (Applied Biosystems). The amount of mRNA was determined relative to that from control samples.

2.7 Data analysis

All experiments with HEK293 and HepaRG cells were performed in triplicates (with a couple of exceptions), while the experiments on oocytes were performed in triplicates or more. The values were expressed as mean \pm standard deviation.

The active uptake was calculated as the difference in mean values of test and control experiments.

Kinetic constants (K_m and V_{max}) for carrier-mediated uptake were estimated by fitting the calculated uptake data to the Michaelis-Menten model (equation 1.4) without weighting (XLfit4 Excel Add-In v.4.2.2 software, Microsoft). The results from the analyses were given as point estimates of the K_m and V_{max} values \pm standard error.

3 RESULTS

3.1 Time dependence uptake studies

3.1.1 HEK293 cells

Estradiol-17 β -D-glucuronide

The time course of uptake of [3 H]estradiol-17 β -D-glucuronide at a low concentration (3.8 nM, 0.2 μ Ci/ml) by HEK293 cells is shown in Figure 3.1. The carrier-mediated uptake of estradiol-17 β -D-glucuronide in HEK293/OATP1B1 increased linearly up to approximately 300 seconds. The uptake ratio was 2.3 at 60 seconds, the time of incubation used in the concentration dependence studies. The intracellular amount of substrate at 900 seconds was 1.5% of initial amount in the test solution.

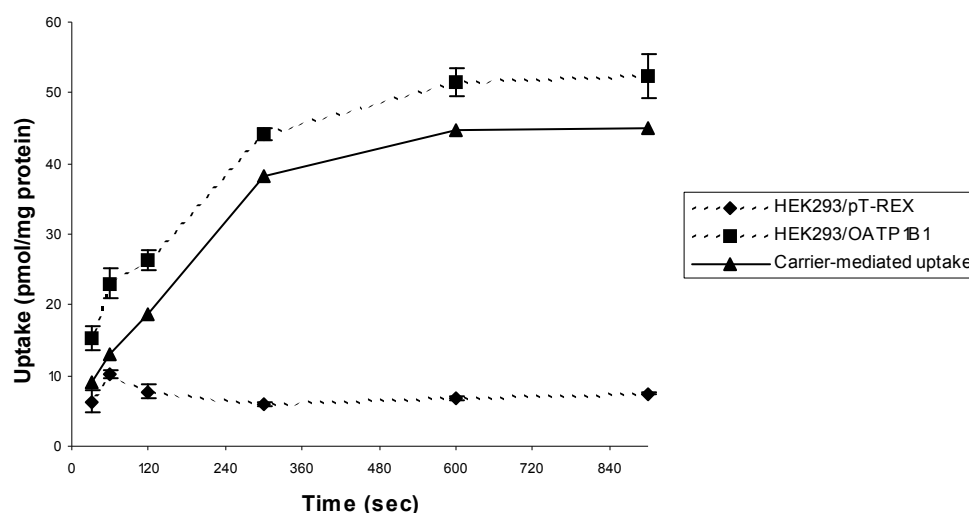


Figure 3.1 Time course of [3 H]estradiol-17 β -D-glucuronide (3.8 nM) uptake in HEK293 cells transfected with OATP1B1 (\blacksquare) and vector-transfected control cells, HEK293/pT-REX (\blacklozenge). The triangles (\blacktriangle) represent the carrier-mediated uptake in the OATP1B1-expressing HEK293 cells. Each point represents the mean \pm S.D. (n=3).

The time course of uptake of estradiol-17 β -D-glucuronide at a high concentration (50 μ M, 1 μ Ci/ml) by HEK293 cells is shown in Figure 3.2. The carrier-mediated uptake of estradiol-17 β -D-glucuronide in HEK293/OATP1B1 increased linearly up to approximately 90 seconds. The uptake ratio was 3.7 at 60 seconds, the time of incubation used in the concentration dependence studies.

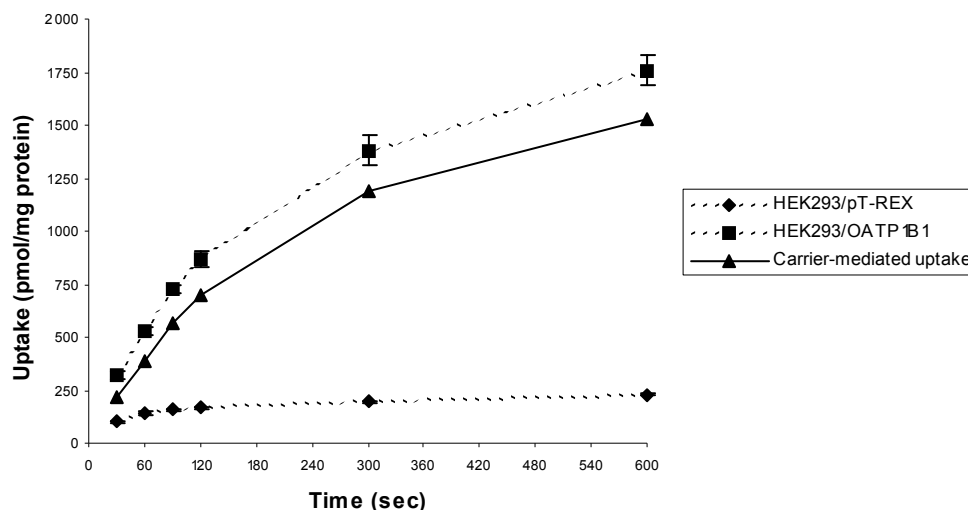


Figure 3.2 Time course of estradiol-17 β -D-glucuronide (50 μ M) uptake in HEK293 cells transfected with OATP1B1 (\blacksquare) and vector-transfected control cells, HEK293/pT-REX (\blacklozenge). The triangles (\blacktriangle) represent the carrier-mediated uptake in the OATP1B1-expressing HEK293 cells. Each point represents the mean \pm S.D. (n=3).

Atorvastatin

The time course of uptake of [3 H]atorvastatin (80 nM, 0.4 μ Ci/ml) by HEK293 cells is shown in Figure 3.3. The carrier-mediated uptake of atorvastatin in HEK293/OATP1B1 increased linearly up to approximately 45 seconds. The uptake ratio was 6.4 at 60 seconds, the time of incubation used in the concentration dependence studies. The intracellular amount of substrate at 600 seconds was 4.3% of initial amount in the test solution.

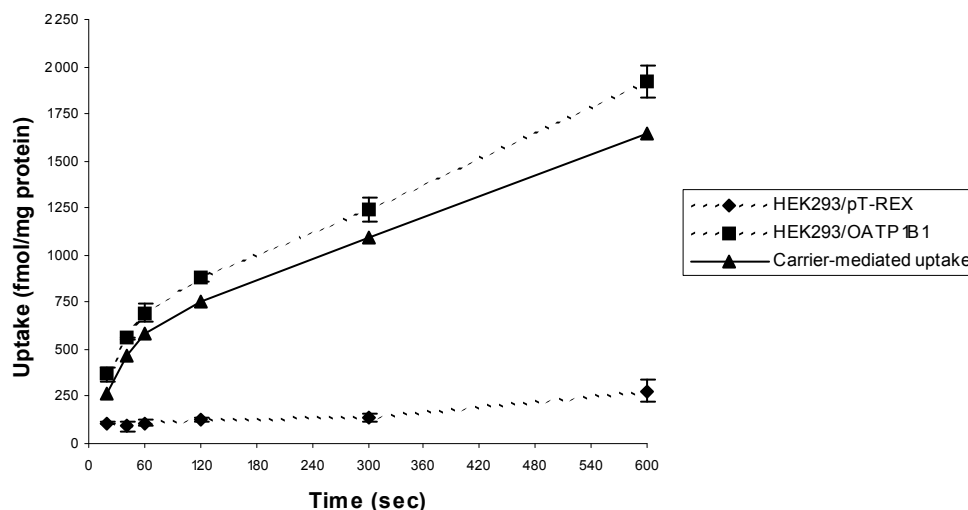


Figure 3.3 Time course of [3 H]atorvastatin (80 nM) uptake in HEK293 cells transfected with OATP1B1 (\blacksquare) and vector-transfected control cells, HEK293/pT-REX (\blacklozenge). The triangles (\blacktriangle) represent the carrier-mediated uptake in the OATP1B1-expressing HEK293 cells. Each point represents the mean \pm S.D. (n=2).

Results from a time dependence uptake study with atorvastatin performed during the testing of conditions are shown in Appendix 1. The conditions used in the experiment are shown in the appendix. The uptake ratio in this experiment was 1.8 at 60 seconds (Figure 7.1).

Pravastatin

The time course of uptake of [^3H]pravastatin (50 nM, 1 $\mu\text{Ci/ml}$) by HEK293 cells is shown in Figure 3.4. The carrier-mediated uptake of pravastatin in HEK293/OATP1B1 increased linearly up to approximately 60 seconds. The uptake ratio was 13.4 at 60 seconds, the time of incubation used in the concentration dependence studies. The intracellular amount of substrate at 600 seconds was 4.9% of initial amount in the test solution.

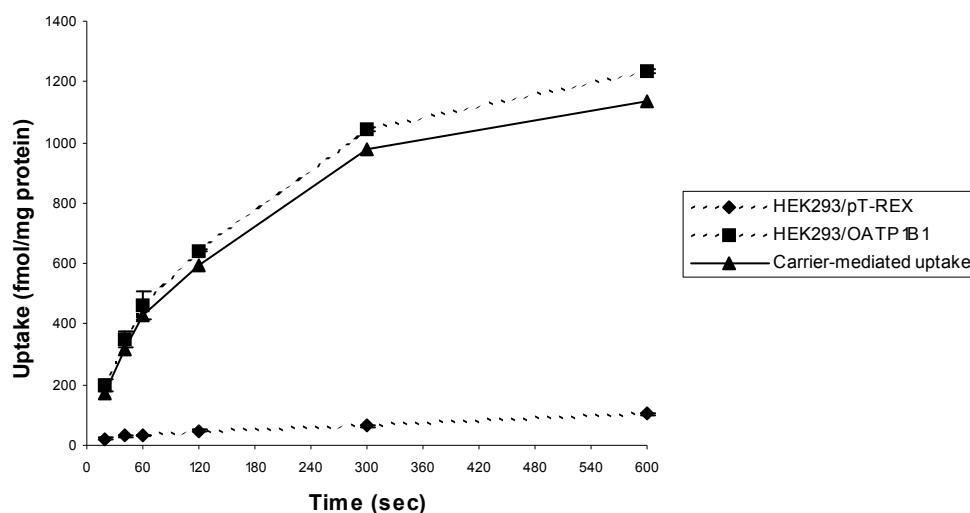


Figure 3.4 Time course of [^3H]pravastatin (50 nM) uptake in HEK293 cells transfected with OATP1B1 (■) and vector-transfected control cells, HEK293/pT-REX (◆). The triangles (▲) represent the carrier-mediated uptake in the OATP1B1-expressing HEK293 cells. Each point represents the mean \pm S.D. (n=2).

Results from time dependence uptake studies with pravastatin performed during the testing of conditions are shown in Appendix 2. The conditions used in the experiments are shown in the appendix. The uptake ratios in these experiments were 1.9 (Figure 7.2) and 1.6 (Figure 7.3) at 60 seconds. In the experiment where the cells were treated with sodium butyrate 24 hours prior to experimentation, the uptake ratio was 1.3 at 60 seconds (Figure 7.4).

3.1.2 Hepa RG cells

Estradiol-17 β -D-glucuronide

The time course of uptake of [^3H]estradiol-17 β -D-glucuronide (19 nM, 1 $\mu\text{Ci/ml}$) by HepaRG cells at 37°C and 4°C is shown in Figure 3.5. The carrier-mediated uptake of estradiol-17 β -D-glucuronide increased linearly up to approximately 60 seconds. The uptake ratio was 2.0 at 60 seconds, the time of incubation used in the concentration dependence studies. The intracellular amount of substrate at 600 seconds was 1.4% of initial amount in the test solution.

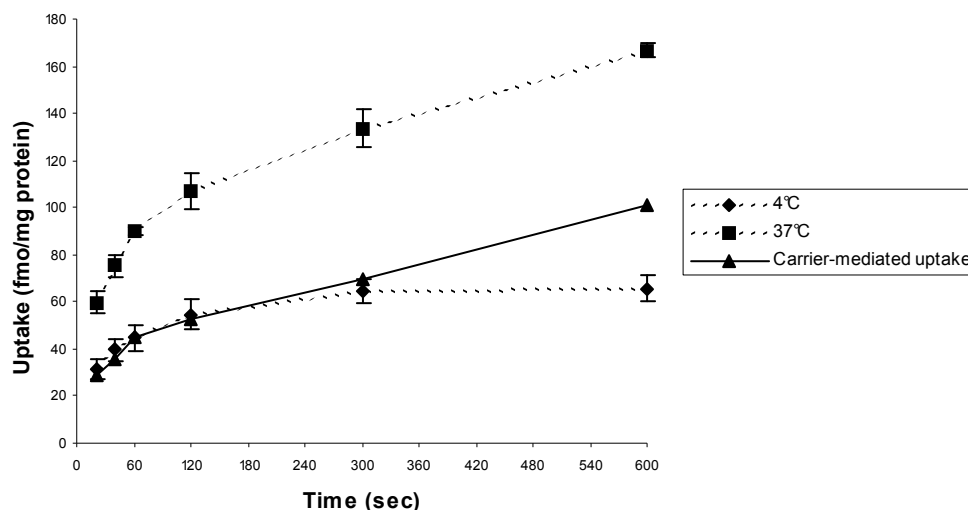


Figure 3.5 Time course of uptake of [³H]estradiol-17β-D-glucuronide (19 nM) by HepaRG cells at 37°C (■) and 4°C (◆). The triangles (▲) represent the carrier-mediated uptake in the HepaRG cells. Each point represents the mean ± S.D. (n=3).

Atorvastatin

The time course of uptake of [³H]atorvastatin (80 nM, 0.4 μCi/ml) by HepaRG cells at 37°C and 4°C is shown in Figure 3.6. The carrier-mediated uptake of atorvastatin increased linearly up to approximately 60 seconds. The uptake ratio was 9.1 at 60 seconds, the time of incubation used in the concentration dependence studies. The intracellular amount of substrate at 600 seconds was 14.4% of initial amount in the test solution. It should be noted that this experiment was performed with only one replicate.

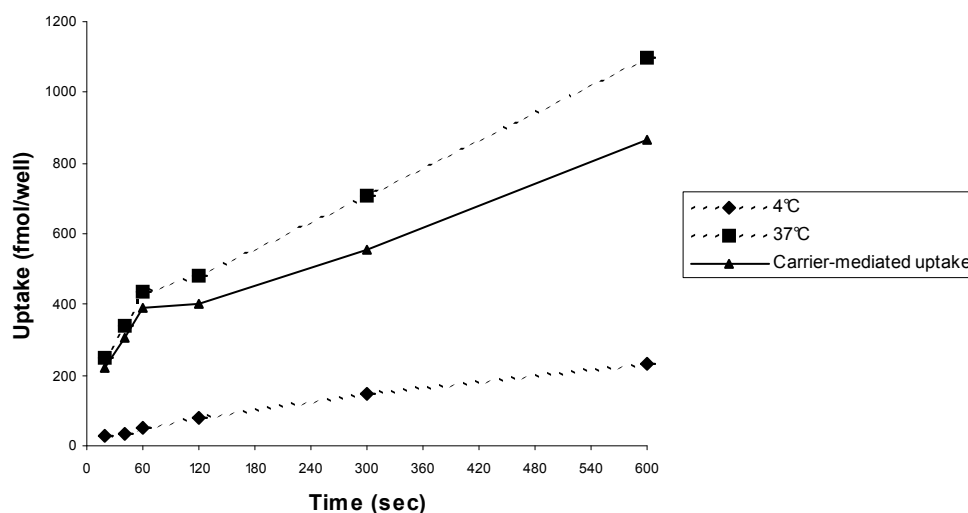


Figure 3.6 Time course of uptake of [³H]atorvastatin (80 nM) by HepaRG cells at 37°C (■) and 4°C (◆). The triangles (▲) represent the carrier-mediated uptake in the HepaRG cells. Each point represents one value (n=1).

Pravastatin

The time course of uptake of [3 H]pravastatin (50 nM, 1 μ Ci/ml) by HepaRG cells at 37°C and 4°C is shown in Figure 3.7. The carrier-mediated uptake of pravastatin increased linearly up to approximately 300 seconds. The uptake ratio was 4.2 at 60 seconds, the time of incubation used in the concentration dependence studies. The intracellular amount of substrate at 600 seconds was 0.48% of initial amount in the test solution. It should be noted that this experiment was performed with only one replicate.

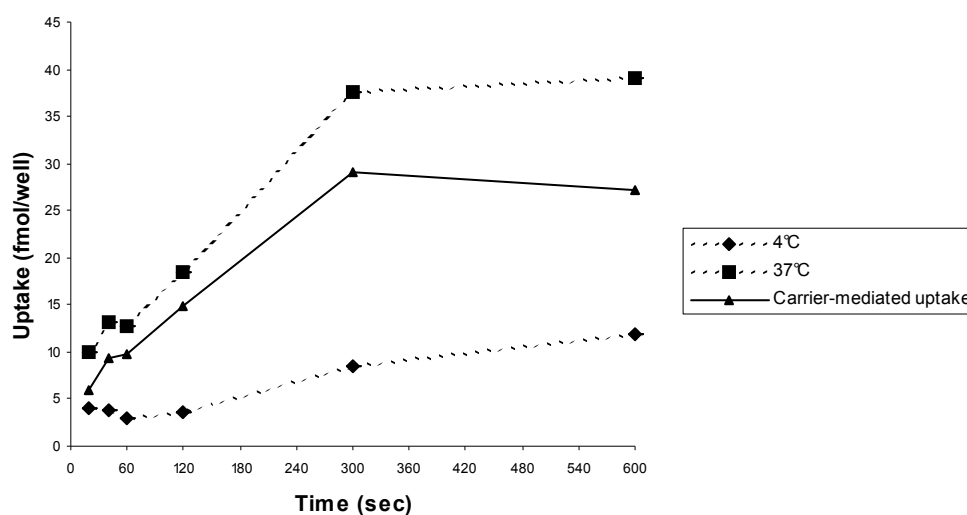


Figure 3.7 Time course of uptake of [3 H]pravastatin (50 nM) by HepaRG cells at 37°C (■) and 4°C (◆). The triangles (▲) represent the carrier-mediated uptake in the HepaRG cells. Each point represents one value (n=1).

3.1.3 *Xenopus laevis* oocytes

Estradiol-17 β -D-glucuronide

The time course of uptake of [3 H]estradiol-17 β -D-glucuronide (1 μ M, 46.9 μ Ci/ml) by oocytes injected with OATP1B1 cRNA and oocytes injected with water is shown in Figure 3.8. The carrier-mediated uptake of estradiol-17 β -D-glucuronide increased linearly up to approximately 60 minutes. The uptake ratio was 31.7 at 60 minutes, the time of incubation used in the concentration dependence studies.

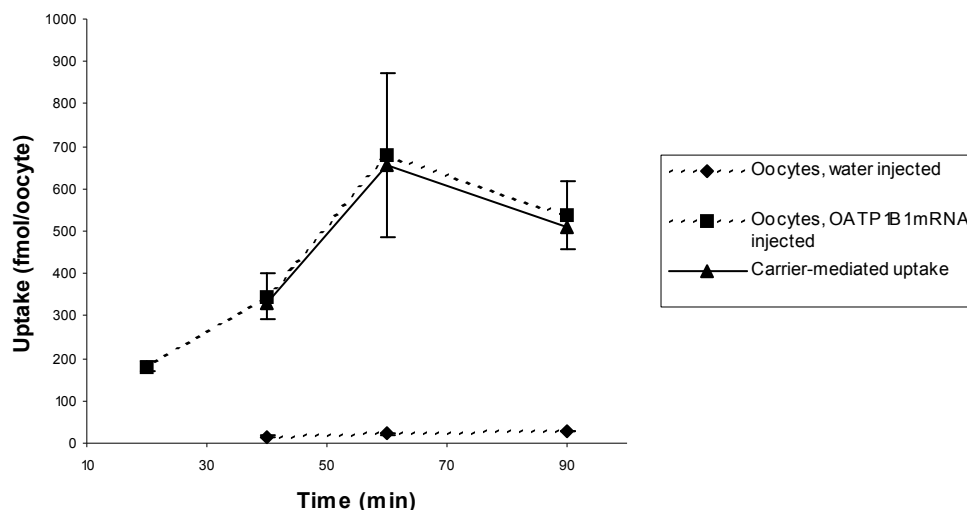


Figure 3.8 Time course of [^3H]estradiol-17 β -D-glucuronide (1 μM) uptake in *Xenopus laevis* oocytes injected with OATP1B1 cRNA (■) and water injected control oocytes (◆). The triangles (▲) represent the carrier-mediated uptake in the OATP1B1-expressing oocytes. Each point represents the mean \pm S.D. (n=3).

The reason why there is no value for the uptake in water injected oocytes at 20 minutes is that all the oocytes were washed away by a mistake during the experiment. From the curve (Figure 3.8) we can assume that the uptake in the water injected oocytes are linear up to 90 minutes, and therefore that the carrier-mediated uptake is linear up to 60 minutes.

Atorvastatin

The time course of uptake of [^3H]atorvastatin (1 μM , 5 $\mu\text{Ci/ml}$) by oocytes injected with OATP1B1 cRNA and oocytes injected with water is shown in Figure 3.9. The carrier-mediated uptake of atorvastatin increased linearly up to 90 minutes. The uptake ratio was 2.7 at 60 minutes, the time of incubation used in the concentration dependence studies.

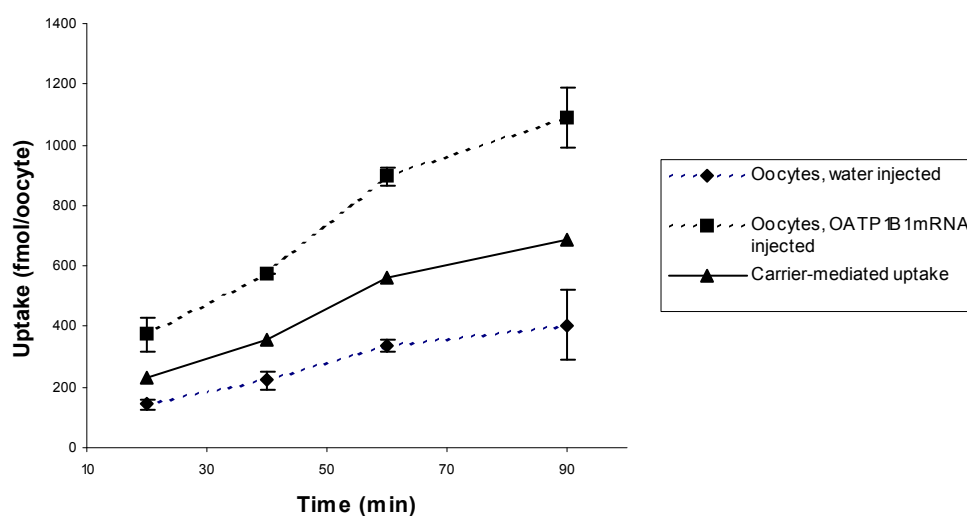


Figure 3.9 Time course of [^3H]atorvastatin (1 μM) uptake in *Xenopus laevis* oocytes injected with OATP1B1 cRNA (■) and water injected control oocytes (◆). The triangles (▲) represent the carrier-mediated uptake in the OATP1B1-expressing oocytes. Each point represents the mean \pm S.D. (n=3).

Pravastatin

The time course of uptake of [^3H]pravastatin ($1\ \mu\text{M}$, $20\ \mu\text{Ci/ml}$) by oocytes injected with OATP1B1 cRNA and oocytes injected with water is shown in Figure 3.10. The carrier-mediated uptake of pravastatin was limited increased linearly up to 90 minutes. The uptake ratio was very low (1.1 at 60 minutes), indicating a limited active uptake.

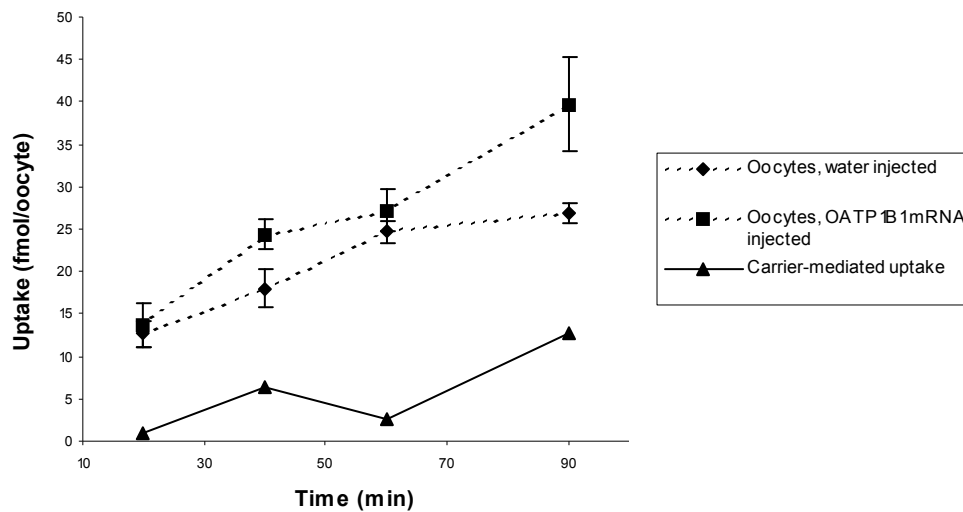


Figure 3.10 Time course of [^3H]pravastatin ($1\ \mu\text{M}$) uptake in *Xenopus laevis* oocytes injected with OATP1B1 cRNA (\blacksquare) and water injected control oocytes (\blacklozenge). The triangles (\blacktriangle) represent the carrier-mediated uptake in the OATP1B1-expressing oocytes. Each point represents the mean \pm S.D. ($n=3$).

3.2 Concentration dependence uptake studies

3.2.1 HEK293 cells

Estradiol-17 β -D-glucuronide

Concentration dependence of the initial uptake rate of estradiol-17 β -D-glucuronide (0.5-75 μ M, 0.938 μ Ci/ml) in HEK293 cells transfected with OATP1B1 and pT-REX is shown in Figure 3.11. Time of incubation was set to 60 seconds based on results from the time dependence uptake studies (Figure 3.1 and 3.2).

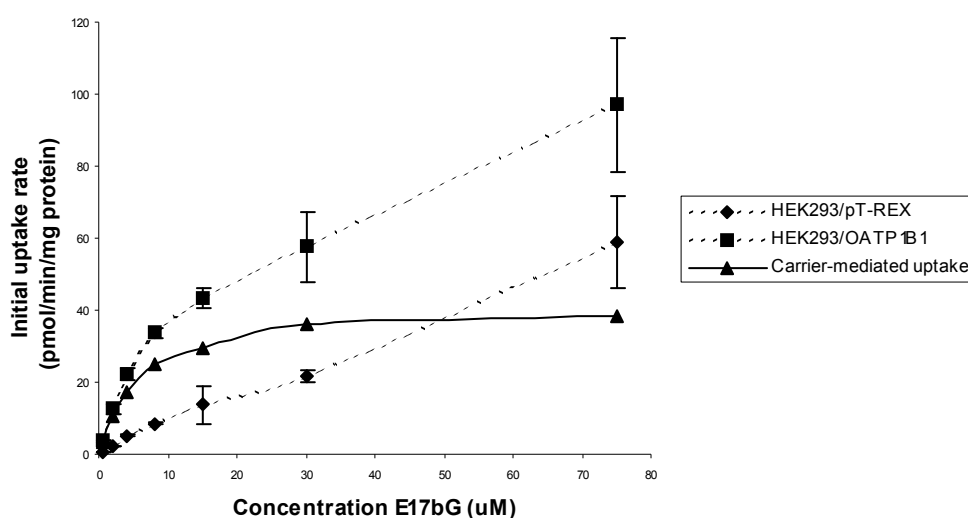


Figure 3.11 Concentration dependence of the initial uptake rate of estradiol-17 β -D-glucuronide in HEK293 cells transfected with OATP1B1 (\blacksquare) and vector-transfected control cells, HEK293/pT-REX (\blacklozenge). The triangles (\blacktriangle) represent the carrier-mediated uptake in the OATP1B1-expressing HEK293 cells. Each point represents the mean \pm S.D. (n=3).

The active transport of estradiol-17 β -D-glucuronide into HEK293/OATP1B1 was saturated. Kinetic analysis estimated K_m and V_{max} values of $5.6 \pm 0.3 \mu$ M and 41.5 ± 0.7 pmol/min/mg protein, respectively (Figure 3.12). This K_m value was approximately ten times lower than in similar experiments performed during testing of culturing and seeding conditions (Appendix 3). The K_m values ranged from 43.9 – 77.4 μ M in the initial testing (Figure 7.5 – 7.10), but none of the variables tested showed a consistent change in K_m value.

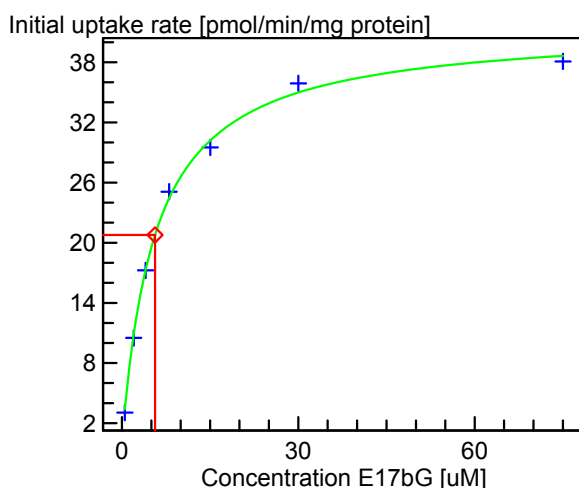


Figure 3.12 The carrier-mediated uptake of estradiol-17 β -D-glucuronide in HEK293/OATP1B1 cells after fitting the uptake data to the modified Michaelis-Menten model (Equation 1.4) The dotted line indicates the estimated K_m value; the substrate concentration at $\frac{1}{2} V_{max}$ (Figure 1.8).

Results from concentration dependence uptake studies where the test solutions in the dilution series contained different amount of radiolabeled compound are shown in Appendix 4. Kinetic analysis of these results estimated K_m values of $64.4 \pm 4.6 \mu\text{M}$ and $48.0 \pm 8.8 \mu\text{M}$ (Figure 7.11 and 7.12). These results were similar to results from corresponding experiments where the test solutions in the dilution series contained the *same* amount of radiolabeled compound.

Atorvastatin

Concentration dependence of the initial uptake rate of atorvastatin (1-300 μM , 0.6 $\mu\text{Ci/ml}$) in HEK293 cells transfected with OATP1B1 and pT-REX is shown in Figure 3.13. Time of incubation should be set to 45 seconds based on results from the time dependence uptake study (Figure 3.3). Due to limitations of the experimentation assay the time was set to 60 seconds. It is practically impossible to perform the experiment with a time of incubation less than 60 seconds. The uptake of atorvastatin into HEK293/OATP1B1 and HEK293/pT-REX was both linear, and the uptake ratio was approximately 1 in the entire concentration range.

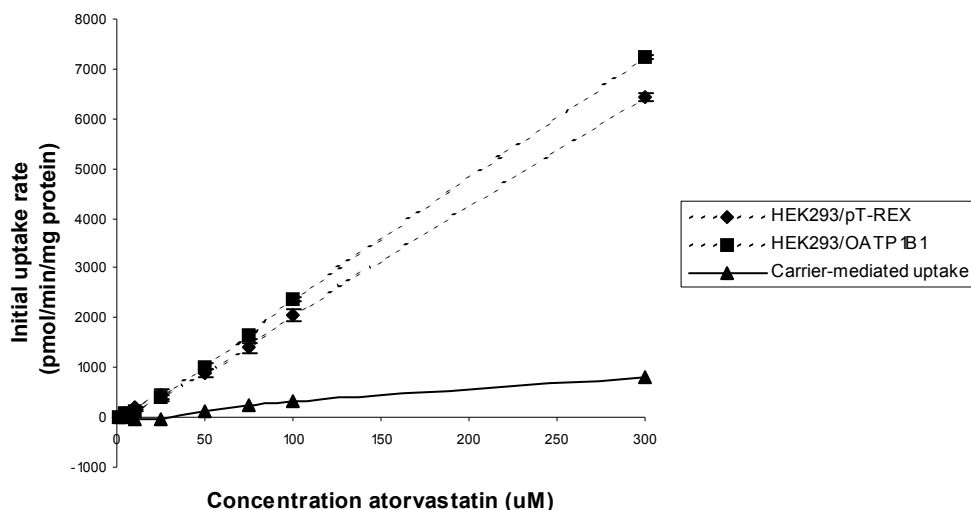


Figure 3.13 Concentration dependence of the initial uptake rate of atorvastatin in HEK293 cells transfected with OATP1B1 (■) and vector-transfected control cells, HEK293/pT-REX (◆). The triangles (▲) represent the carrier-mediated uptake in the OATP1B1-expressing HEK293 cells. Each point represents the mean \pm S.D. (n=3).

Pravastatin

Concentration dependence of the initial uptake rate of pravastatin (1-300 μ M, 1 μ Ci/ml) in HEK293 cells transfected with OATP1B1 and pT-REX is shown in Figure 3.14. Time of incubation was set to 60 seconds based on results from the time dependence uptake study (Figure 3.4). The uptake into HEK293/OATP1B1 and HEK293/pT-REX was both linear, and the uptake ratio was approximately 1 in the entire concentration range.

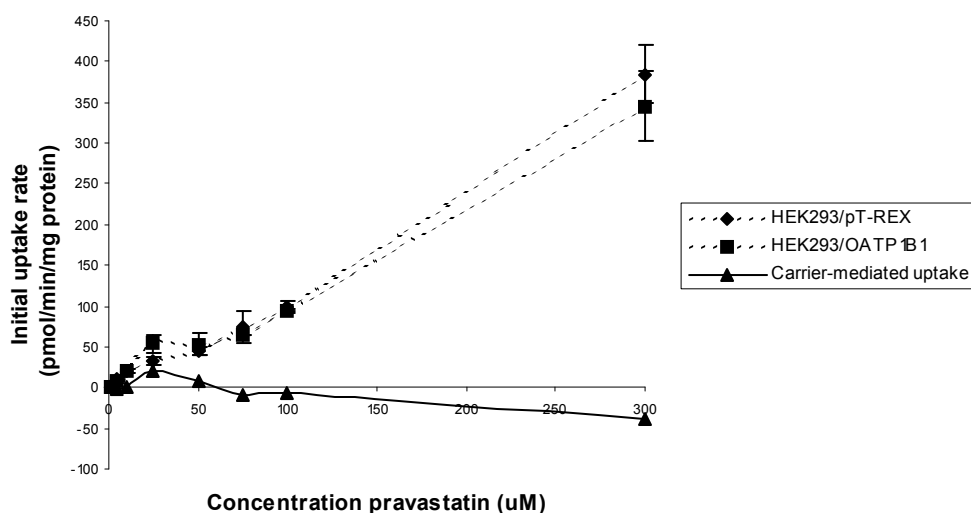


Figure 3.14 Concentration dependence of the initial uptake rate of pravastatin in HEK293 cells transfected with OATP1B1 (■) and vector-transfected control cells, HEK293/pT-REX (◆). The triangles (▲) represent the carrier-mediated uptake in the OATP1B1-expressing HEK293 cells. Each point represents the mean \pm S.D. (n=3).

3.2.2 HepaRG cells

Estradiol-17 β -D-glucuronide

Concentration dependence of the initial uptake rate of estradiol-17 β -D-glucuronide (0.5-75 μ M, 0.938 μ Ci/ml) in HepaRG cells at 37 $^{\circ}$ C and 4 $^{\circ}$ C is shown in Figure 3.15. Time of incubation was set to 60 seconds based on results from the time dependence uptake studies (Figure 3.5).

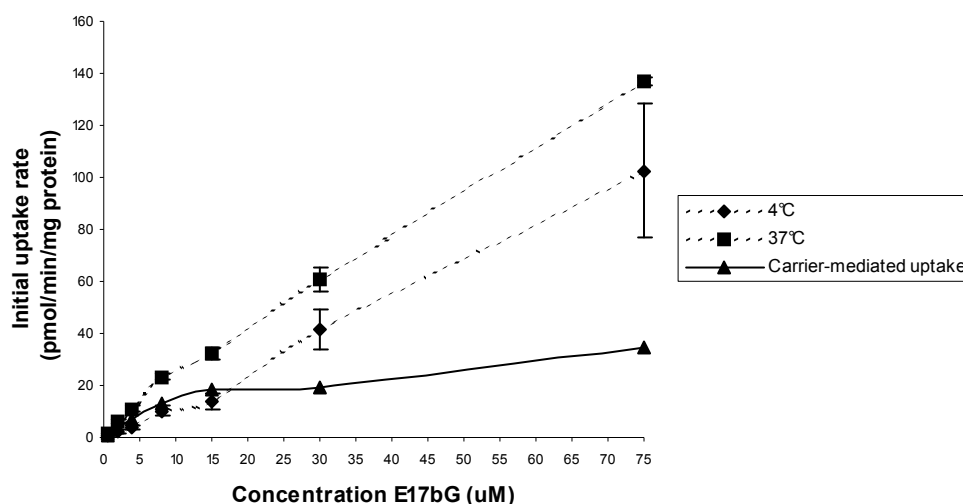


Figure 3.15 Concentration dependence of the initial uptake rate of estradiol-17 β -D-glucuronide in HepaRG cells at 37 $^{\circ}$ C (\blacksquare) and 4 $^{\circ}$ C (\blacklozenge). The triangles (\blacktriangle) represent the carrier-mediated uptake in the HepaRG cells. Each point represents the mean \pm S.D. (n=3).

The active transport of estradiol-17 β -D-glucuronide into HepaRG cells was saturated. Kinetic analysis estimated K_m and V_{max} values of 22.3 ± 7.1 μ M and 41.9 ± 5.6 pmol/min/mg protein, respectively (Figure 3.16).

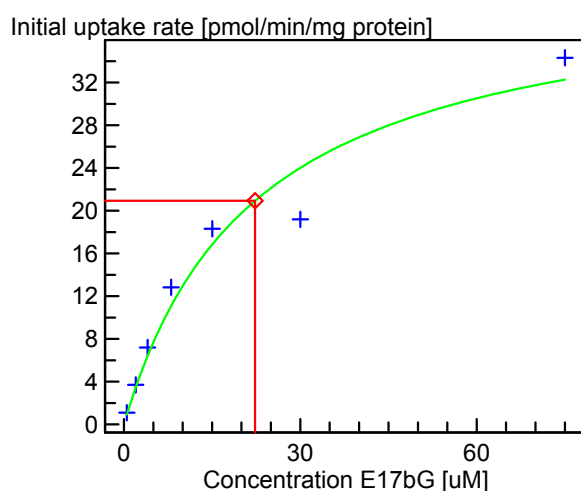


Figure 3.16 The carrier-mediated uptake of estradiol-17 β -D-glucuronide in HepaRG cells after fitting the uptake data to the modified Michaelis-Menten model (Equation 1.4). The dotted line indicates the estimated K_m value; the substrate concentration at $\frac{1}{2} V_{max}$ (Figure 1.8).

Atorvastatin

Concentration dependence of the initial uptake rate of atorvastatin (1-300 μM , 0.4 $\mu\text{Ci/ml}$) in HepaRG cells at 37°C and 4°C is shown in Figure 3.17. Time of incubation was set to 60 seconds based on results from the time dependence uptake study (Figure 3.6).

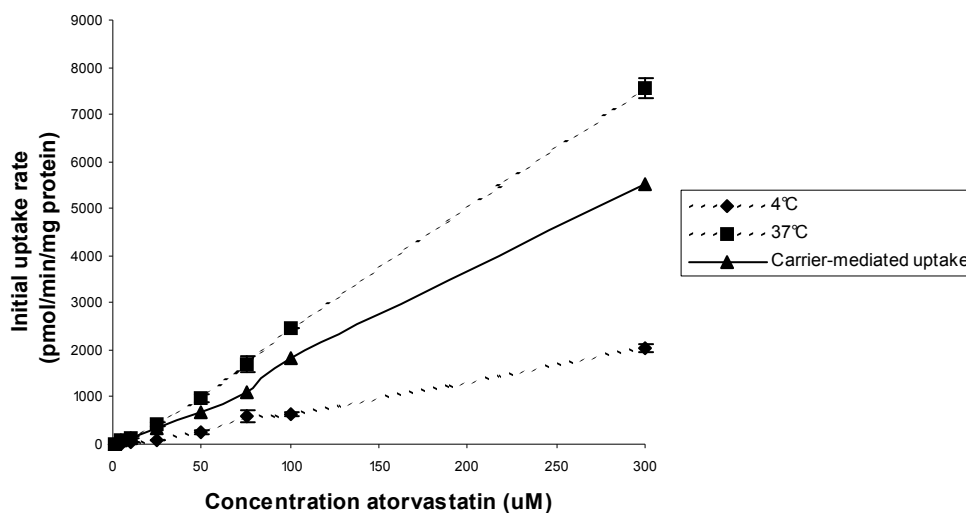


Figure 3.17 Concentration dependence of the initial uptake rate of atorvastatin in HepaRG cells at 37°C (■) and 4°C (◆). The triangles (▲) represent the carrier-mediated uptake in the HepaRG cells. Each point represents the mean \pm S.D. (n=3).

The active transport of atorvastatin into HepaRG cells was not saturated. The uptake of atorvastatin was linear at both 37°C and 4°C, with an uptake ratio around 4 in the entire concentration range.

Pravastatin

Concentration dependence of the initial uptake rate of pravastatin (1-300 μM , 1 $\mu\text{Ci/ml}$) in HepaRG cells at 37°C and 4°C is shown in Figure 3.18. Time of incubation was set to 60 seconds based on results from the time dependence uptake study (Figure 3.7). The uptake of atorvastatin into HepaRG cells was linear at both 37°C and 4°C, and the uptake ratio was approximately 1 in the entire concentration range.

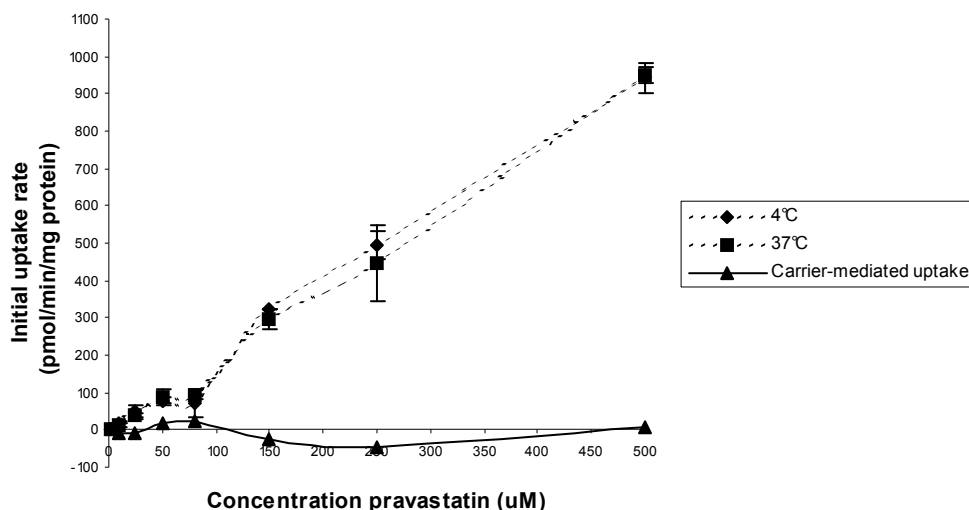


Figure 3.18 Concentration dependence of the initial uptake rate of pravastatin in HepaRG cells at 37°C (■) and 4°C (◆). The triangles (▲) represent the carrier-mediated uptake in the HepaRG cells. Each point represents the mean \pm S.D. (n=3).

3.2.3 *Xenopus laevis* oocytes

Estradiol-17 β -D-glucuronide

Concentration dependence of the initial uptake rate of estradiol-17 β -D-glucuronide (0.5-75 μ M, 46.9 μ Ci/ml) in oocytes injected with OATP1B1 cRNA and water is shown in Figure 3.19. Time of incubation was set to 60 minutes based on results from the time dependence uptake studies (Figure 3.8).

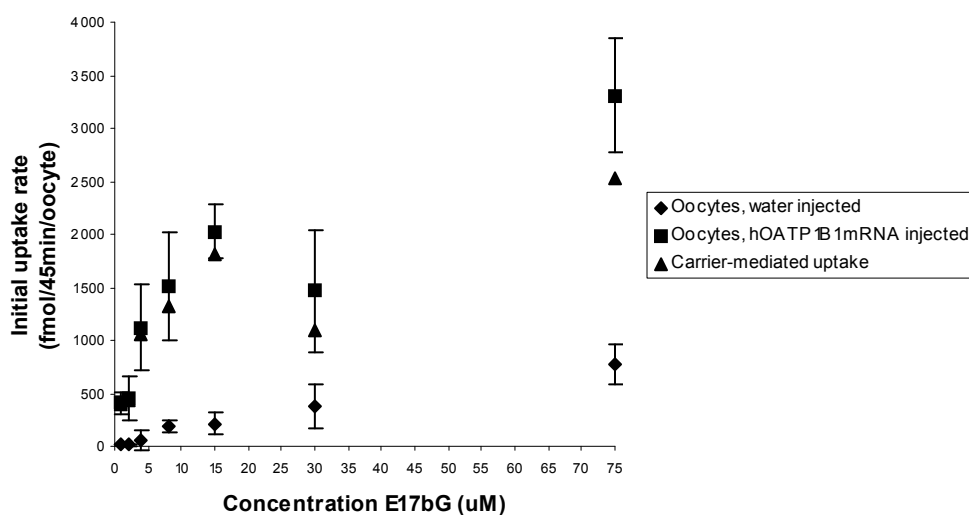


Figure 3.19 Concentration dependence of the initial uptake rate of estradiol-17 β -D-glucuronide in *Xenopus laevis* oocytes injected with OATP1B1 cRNA (■) and water injected control oocytes (◆). The triangles (▲) represent the carrier-mediated uptake in the oocytes expressing OATP1B1. Each point represents the mean \pm S.D. (n=8).

The active transport of estradiol-17 β -D-glucuronide into oocytes/OATP1B1 was saturated. Kinetic analysis estimated K_m and V_{max} values of $5.9 \pm 3.8 \mu\text{M}$ and $2236.1 \pm 432.2 \text{ fmol}/60\text{min}/\text{oocyte}$, respectively (Figure 3.20).

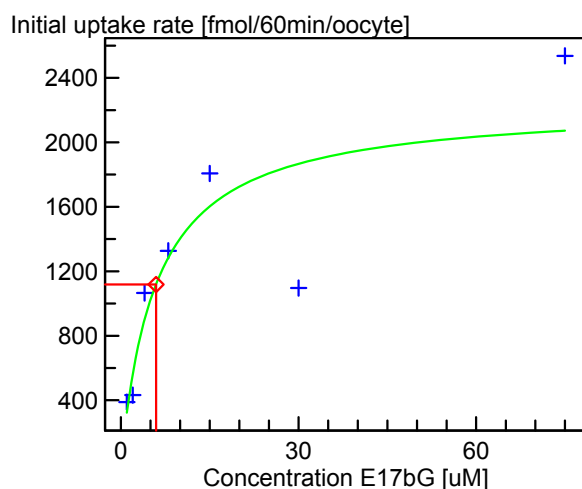


Figure 3.20 The carrier-mediated uptake of estradiol-17 β -D-glucuronide in oocytes expressing OATP1B1 after fitting the uptake data to the modified Michaelis-Menten model (Equation 1.4). The dotted line indicates the estimated K_m value; the substrate concentration at $\frac{1}{2} V_{max}$ (Figure 1.8).

Atorvastatin

Concentration dependence of the initial uptake rate of atorvastatin (1-300 μM , 5 $\mu\text{Ci}/\text{ml}$) in oocytes injected with OATP1B1 cRNA and water is shown in Figure 3.21. Time of incubation was set to 60 minutes based on results from the time dependence uptake studies (Figure 3.9).

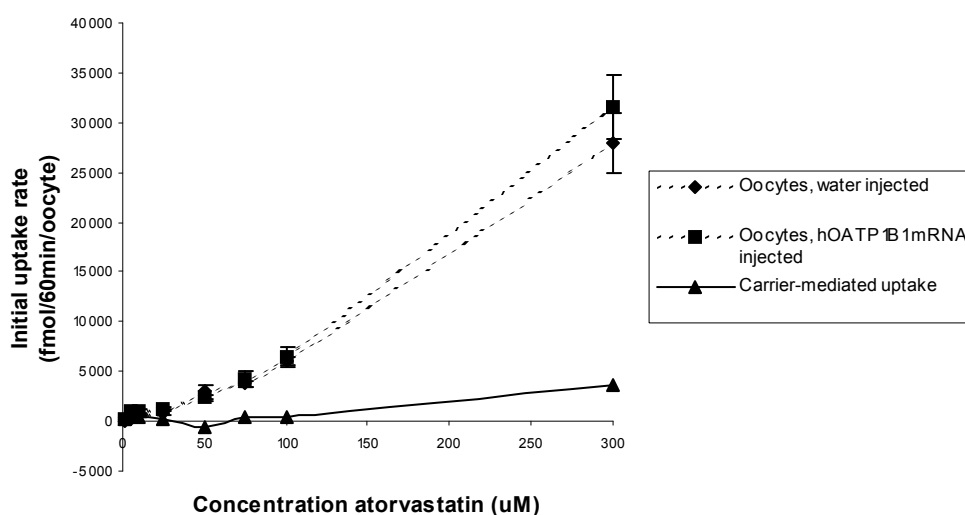


Figure 3.21 Concentration dependence of the initial uptake rate of atorvastatin in *Xenopus laevis* oocytes injected with OATP1B1 cRNA (■) and water injected control oocytes (◆). The triangles (▲) represent the carrier-mediated uptake in the oocytes expressing OATP1B1. Each point represents the mean \pm S.D. ($n=6-7$).

The uptake of atorvastatin into oocytes/OATP1B1 and control oocytes was both linear, and the uptake ratio was approximately 1 in the entire concentration range.

Pravastatin

Concentration dependence of the initial uptake rate of pravastatin (1-250 μM , 20 $\mu\text{Ci/ml}$) in oocytes injected with OATP1B1 cRNA and water is shown in Figure 3.22. Time of incubation was set to 60 minutes based on results from the time dependence uptake studies (Figure 3.10).

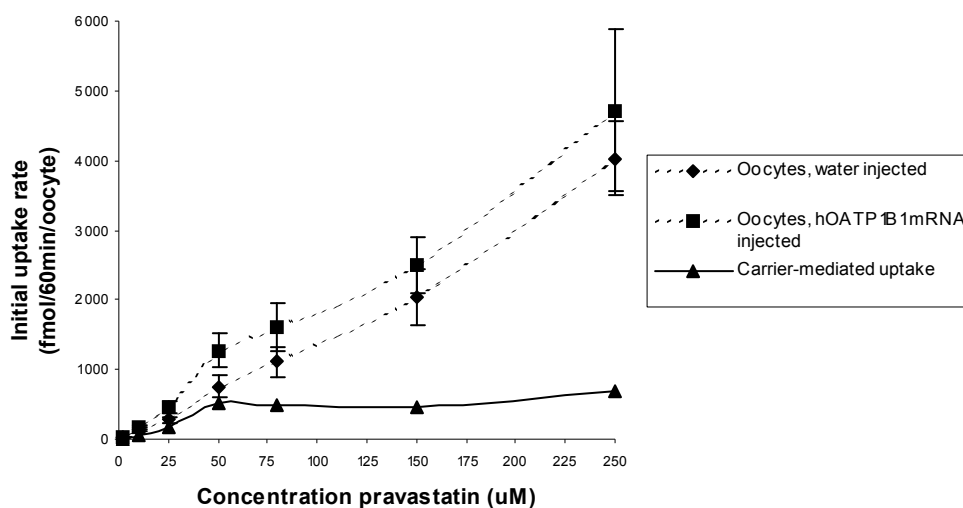


Figure 3.22 Concentration dependence of the initial uptake rate of pravastatin in *Xenopus laevis* oocytes injected with OATP1B1 cRNA (■) and water injected control oocytes (◆). The triangles (▲) represent the carrier-mediated uptake in the oocytes expressing OATP1B1. Each point represents the mean \pm S.D. (n=6-7).

The active transport of pravastatin into oocytes/OATP1B1 was saturated. Kinetic analysis estimated K_m and V_{max} values of $54.8 \pm 31.4 \mu\text{M}$ and $791.9 \pm 162.5 \text{ fmol/60min/oocyte}$, respectively (Figure 3.23).

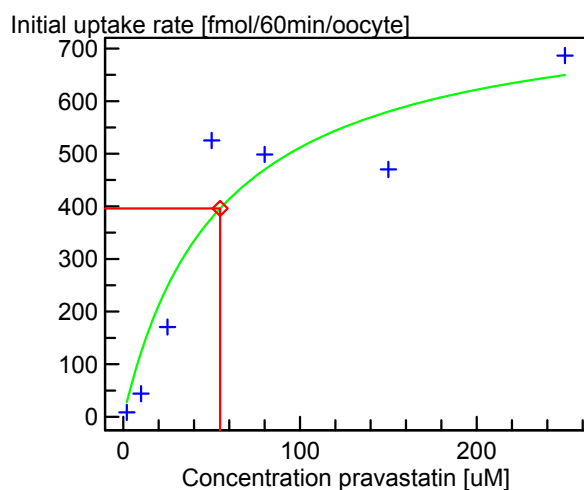


Figure 3.23 The carrier-mediated uptake of pravastatin in oocytes expressing OATP1B1 after fitting the uptake data to the modified Michaelis-Menten model (Equation 1.4.) The dotted line expresses the estimation of the K_m value; the substrate concentration at $\frac{1}{2} V_{max}$ (Figure 1.8).

3.3 mRNA quantification

Results from the comparison of total amount of OATP1B1 mRNA in HEK293/OATP1B1 cells, HEK293/pT-REX cells, and HEK293/OATP1B1 cells treated with Na-butyrate, are shown in Figure 3.24. The amount of OATP1B1 mRNA in the HEK/pT-REX cells was not detectable. Treatment with sodium butyrate gave no significant change ($p \sim 0.21$) in the amount of OATP1B1 mRNA in the HEK293/OATP1B1 cells.

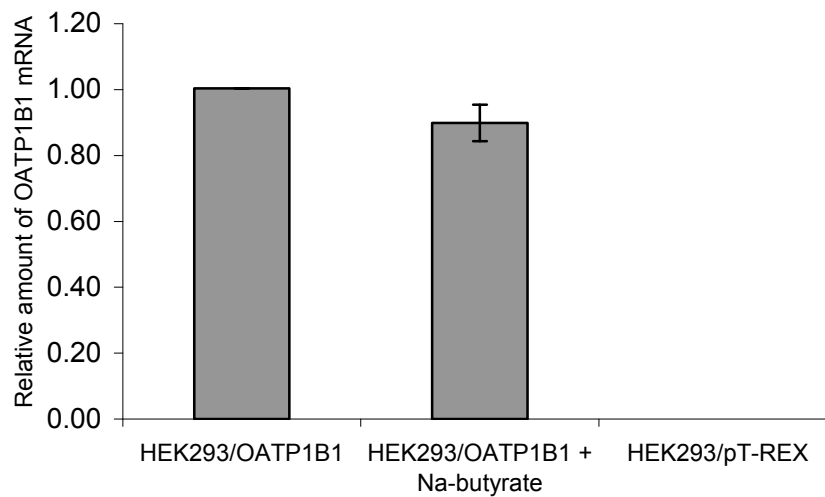


Figure 3.24 Relative amount of OATP1B1 mRNA in HEK293/OATP1B1 cells treated with sodium butyrate and in HEK293/pT-REX cells, compared to HEK293/OATP1B1 cells. Values are calculated with untreated HEK293/OATP1B1 cells as reference and results are shown as mean \pm S.D. ($n=3$). The amount of OATP1B1 mRNA is normalized to PPIA mRNA and MVP mRNA.

4 DISCUSSION

4.1 Methodological considerations

Transfected HEK293 cells is the most applied system for determination of whether a compound is a substrate of OATP1B1, while estradiol-17 β -D-glucuronide is the best recognized substrate of the OATP1B1 transporter. In the preliminary experiments, the intention was to reproduce results from prior uptake studies on HEK293 cells with the estradiol-17 β -D-glucuronide (Table 4.1). However, the estimated K_m value of the initial experiments ($\sim 70 \mu\text{M}$) was approximately 10-fold higher than previously published values ($\sim 4\text{--}8 \mu\text{M}$) (Table 4.1). The results showed that changes in culture medium, amount of medium and cells seeded per flask, frequency of splitting, trypsination, laboratory, and cells subcultivated at different AstraZeneca sites, had a limited impact on the estimated K_m value of estradiol-17 β -D-glucuronide ($\sim 45\text{--}65 \mu\text{M}$). In a single experiment, a K_m value of $5.6 \mu\text{M}$ was obtained (Figure 3.12). In this experiment, it was observed reduced cell confluency in the wells before experimentation. The amount of cells seeded three days prior to experimentation was the same as in previous studies, but these specific cells (from a certain vial) were observed to grow very slowly during the period of splitting and seeding in flasks prior to seeding in 24-well plates.

Reduced cell confluency is consistent with increased surface area per cell exposed to substrate solution. This could explain the more rapid increase in uptake at low concentrations, compared to the uptake in confluent cell layers, and the resulting low K_m value. Reduced amount of cells seeded per well had previously been tested in the process of optimising the method. However, reduction from 0.5 million to 0.3 million cells seeded per well had limited impact on the estimated K_m value of estradiol-17 β -D-glucuronide. The impact of cell confluency in uptake studies with HEK293 cells should be further studied.

In the studies of Iwai et al. and König et al., the HEK293 cells were treated with sodium butyrate prior to experimentation (Iwai et al., 2004; König et al., 2000). Sodium butyrate is supposed to induce the mRNA expression, resulting in increased protein expression (Kruh, 1982). However, sodium butyrate could also induce cell toxicity (Louis et al., 2004). The mRNA level in HEK293 cells after sodium butyrate treatment was reduced rather than increased, which indicates that the cell toxicity induced by sodium butyrate was more important than the induction of OATP1B1.

The intracellular amount of substrate after uptake was low compared to the total amount in the test solution ($<5\%$ in all except from one experiment). It is assumed that the whole extracellular amount of substrate is available for intracellular uptake. However, there is a

possibility that substrate adherence to cell membranes and/or plastic walls of the wells could result in decreased concentration in the test solution. Overall substrate recovery should therefore be performed to ensure that the added test concentration actually is obtained during experimentation.

Of economical reasons, the time dependence uptake studies were performed at low concentrations, with one exception. Studies at a higher concentration would have been useful to ensure linearity in the whole concentration range applied in the concentration dependence uptake studies. In transporter-mediated uptake, factors causing deviation from linearity of the curve are lack of substance or lack of co-factors. At low concentrations, lack of substrate is relevant, while lack of co-factors is relevant at high concentrations. In uptake experiments at low concentrations, the lack of substrate will probably occur before the lack of co-factors. Therefore, the time point chosen based on time dependence uptake studies at low concentrations, should also be within the linear interval of uptake at high concentrations. Time-dependent uptake of estradiol-17 β -D-glucuronide in HEK293 cells was tested at low and high concentrations, and the linear intervals were similar (Figure 3.1 and Figure 3.2).

In the concentration dependence uptake studies, radioactive compounds were diluted with non-labeled compounds. There is a theoretical possibility that the affinity of the compound to the transporter vary between labeled and non-labeled compound. For estradiol-17 β -D-glucuronide, dilution series containing different amount of labeled compound, and dilution series containing the same amount of labeled compound, were applied in parallel experiments. Results from these studies showed no significant difference in uptake kinetics, indicating that the labeled and non-labeled form of estradiol-17 β -D-glucuronide exhibit similar transporter affinity. Theoretically, labeling could influence the affinity of other substrates, depending on the substrate-transporter interactions and which part of the molecule that is labeled.

4.2 Transport studies

The purpose of the present study was to compare OATP1B1-mediated uptake kinetics in three *in vitro* models. For the probe substrate estradiol-17 β -D-glucuronide, the results from time- and concentration dependence studies were consistent (Table 4.1). The experiments showed active uptake of the probe substrate in both time- and concentration dependence studies. The active uptake of estradiol-17 β -D-glucuronide was saturated in all three systems, and the estimated K_m values were within the range of prior publications on similar systems (Table 4.1).

On the contrary, the results from the uptake studies with atorvastatin and pravastatin were not consistent between and within the models. Atorvastatin showed active uptake in time

dependence uptake studies in all three models. However, in the concentration dependence uptake studies atorvastatin exhibited no active uptake in the overexpressed models, while a non-saturated active uptake was demonstrated in the HepaRG cells. These results are not in accordance with literature data on HEK293 cells, where a saturated, active uptake of atorvastatin (K_m value 12.4 μM) has been reported (Table 4.1).

Table 4.1 Summary of the results from time dependence and concentration dependence uptake studies with three different substrates. Estimated K_m values from the concentration dependence studies are compared with literature values for the same substrate in similar models. There are no prior publications concerning uptake kinetics in HepaRG cells. The K_m values referred to are from studies of human hepatocytes (HH) or rat hepatocytes (rH).

Substrate	In model	vitro	Active uptake, time dep	Active uptake, conc dep	K_m (μM)	K_m (μM) prior published
E17bG	HEK293		Yes	Yes	5.6	8.2 ¹ 4.3 ²
E17bG	HepaRG		Yes	Yes	22.3	10.2 ³ (HH)
E17bG	Oocytes		Yes	Yes	5.9	9.7 ³ 3.0 ⁴
Atorvastatin	HEK293		Yes	No	-	12.4 ⁵
Atorvastatin	HepaRG		Yes	Yes	No saturation	-
Atorvastatin	Oocytes		Yes	No	-	-
Pravastatin	HEK293		Yes	No	-	85.7 ⁵ 33.7 ⁶
Pravastatin	HepaRG		Yes	No	-	10.2 ³ (HH) 29.1 ⁷ (rH) 16.5 ⁸ (rH)
Pravastatin	Oocytes		No	Yes	54.8	13.7 ³

Abbreviations: conc dep; concentration dependence, E17bG; estradiol-17 β -D-glucuronide, HH; human hepatocytes, rH; rat hepatocytes, time dep; time dependence.

¹ (Konig et al., 2000)

² (Iwai et al., 2004)

³ (Nakai et al., 2001)

⁴ (Bossuyt et al., 1996)

⁵ (Kameyama et al., 2005)

⁶ (Hsiang et al., 1999)

⁷ (Yamazaki et al., 1993)

⁸ (Nezasa et al., 2003)

For pravastatin, the observations in the time- and concentration dependence uptake studies were contradictory in all models. In the time dependence studies on HEK293 and HepaRG cells, pravastatin exhibited an active uptake, while only a limited active uptake was demonstrated in the oocytes. The concentration dependence uptake studies showed no active uptake in HEK293 and HepaRG cells, and a saturated, active uptake in oocytes with an estimated K_m value of 54.8 μM . This value is relatively consistent with K_m values reported on pravastatin in various models (\sim 12-86 μM) (Table 4.1), but relatively high compared to another K_m value reported on oocytes (\sim 14 μM) (Table 4.1).

The inconsistent results from the studies on atorvastatin and pravastatin regarding active uptake could possibly be explained by variations in the passive diffusion of the substances. The $\log D$ values of pravastatin and atorvastatin are -0.47 and 1.34 , respectively (Ishigami et al., 2001), compared to -2.78 for estradiol-17 β -D-glucuronide (predicted by C-Lab; ACDlogD with pKa correction library v10), indicating that the statins exhibit passive diffusion to a greater extent than estradiol-17 β -D-glucuronide. When the active uptake of a substance is low compared to the passive diffusion (Figure 1.7B), the models would not be sufficiently sensitive to separate the active uptake from the passive uptake. The inconsistent results in the

experiments with pravastatin and atorvastatin could therefore reflect insufficient sensitivity of the models in determining OATP1B1-mediated uptake of lipophilic substrates with greater passive than active transport.

HepaRG cells are expressing a multiplicity of transporters and enzymes (Aninat et al., 2006; Le Vee et al., 2006). Functional expression analysis of HepaRG cells have shown substantial mRNA levels and functional activity of the uptake transporters OATP-C, OATP-B, OCT1 and NTCP, the efflux transporters P-gp, MRP2, MRP3 and BCRP (Le Vee et al., 2006), and the enzymes CYP1A2, 2C9, 2D6, 2E1 and 3A4 (Aninat et al., 2006). Atorvastatin is reported to be substrate of P-gp, MRP2 and CYP3A4 (Chen et al., 2005; Lau et al., 2006; Lennernas, 2003), while pravastatin is substrate of MRP2, P-gp, BCRP and OATP-B (Hirano et al., 2005; Kobayashi et al., 2003; Matsushima et al., 2005; Sasaki et al., 2002). The unsaturated active uptake of atorvastatin, and the inconsistent results between the time- and concentration dependence uptake studies on pravastatin, could therefore be explained by influence of other active processes than OATP1B1-mediated uptake in HepaRG cells. If the purpose of a study is to determine the uptake mediated specifically by OATP1B1, the effects of specific inhibitors of OATP1B1 on the uptake kinetics, or the effects of siRNA knock down or knock out (Tian et al., 2004; Tian et al., 2005), should be determined.

The present study compared three different *in vitro* models. In addition to issues related to uptake kinetics, the models exhibit differences in practical importance. Of the overexpressed systems, transfected HEK293 cells are cheap and easy to seed, sub cultivate and handle. HEK293 cells therefore represent a promising model, but the impact of cell confluency and substrate lipophilicity on uptake kinetics needs to be evaluated. *Xenopus laevis* oocytes are expensive, and the uptake studies are more time consuming and tedious compared to the cell lines. cRNA injected oocytes as transport models could still be useful tools in studies on newly discovered transporters, when no stably transfected cell line is available, but they are not fitted for large-scale transport studies. HepaRG cells, expressing a natural level of OATP1B1, are extremely expensive (715 Euro per 24-well plate). In addition, studies in HepaRG cells require the use of specific inhibitors or siRNA to estimate net OATP1B1-mediated uptake. HepaRG cells are, however, an interesting model in studies of the quantitative importance of different kinetic processes of a drug in hepatocytes.

5 SUMMARY AND CONCLUSION

In this study, three different *in vitro* models expressing the membrane drug transporter OATP1B1 were compared using three known OATP1B1 substrates. Estradiol-17 β -D-glucuronide was the only substrate showing consistent results between the models, and between time- and concentration dependence uptake studies within the same model. Results from the studies with atorvastatin and pravastatin were generally inconsistent between the models. Furthermore, concentration dependence and saturation of uptake was difficult to obtain even if a time dependent uptake was recorded. The inconsistent results with atorvastatin and pravastatin could be due to the higher lipophilicity and greater extent of passive diffusion compared to estradiol-17 β -D-glucuronide. It could therefore be hypothesized that when a substrate exhibits greater passive diffusion than active uptake, the models would not be sufficiently sensitive to separate the active uptake from the passive uptake. As drugs are generally more lipophilic than estradiol-17 β -D-glucuronide, none of the *in vitro* transport models studied are expected to be appropriate for routine screening of new drugs as possible substrates for OATP1B1.

Of the three *in vitro* models studied, transfected HEK293 cells are exhibiting most practical advantages as a transport model for large-scale transport studies. They are cheap, easy to seed and sub cultivate, and easy to handle and work with in uptake studies. However, the impact of seeding density, cell confluency and substrate lipophilicity should be further studied to improve the method.

6 REFERENCES

- Abdul-Ghaffar NU and el-Sonbaty MR (1995) Pancreatitis and rhabdomyolysis associated with lovastatin-gemfibrozil therapy. *J Clin Gastroenterol* 21(4):340-341.
- Abe T, Kakyo M, Tokui T, Nakagomi R, Nishio T, Nakai D, Nomura H, Unno M, Suzuki M, Naitoh T, Matsuno S and Yawo H (1999) Identification of a novel gene family encoding human liver-specific organic anion transporter LST-1. *J Biol Chem* 274(24):17159-17163.
- Aninat C, Piton A, Glaise D, Le Charpentier T, Langouet S, Morel F, Guguen-Guillouzo C and Guillouzo A (2006) Expression of cytochromes P450, conjugating enzymes and nuclear receptors in human hepatoma HepaRG cells. *Drug Metab Dispos* 34(1):75-83.
- Ballantyne CM, Corsini A, Davidson MH, Holdaas H, Jacobson TA, Leitersdorf E, Marz W, Reckless JP and Stein EA (2003) Risk for myopathy with statin therapy in high-risk patients. *Arch Intern Med* 163(5):553-564.
- Bays H (2006) Statin safety: an overview and assessment of the data--2005. *Am J Cardiol* 97(8A):6C-26C.
- Biggs MJ, Bonser RS and Cram R (2006) Localized rhabdomyolysis after exertion in a cardiac transplant recipient on statin therapy. *J Heart Lung Transplant* 25(3):356-357.
- Bossuyt X, Muller M, Hagenbuch B and Meier PJ (1996) Polyspecific drug and steroid clearance by an organic anion transporter of mammalian liver. *J Pharmacol Exp Ther* 276(3):891-896.
- Buxton ILO (2006) Pharmacokinetics and Pharmacodynamics: The Dynamics of Drug Absorption, Distribution, Action, and Elimination, in *Goodman & Gilman's The Pharmacological Basis of Therapeutics* (Brunton LL, Lazo JS and Parker KL eds) pp 1-22, McGraw-Hill Companies, New York.
- Chang JT, Staffa JA, Parks M and Green L (2004) Rhabdomyolysis with HMG-CoA reductase inhibitors and gemfibrozil combination therapy. *Pharmacoepidemiol Drug Saf* 13(7):417-426.
- Chen C, Mireles RJ, Campbell SD, Lin J, Mills JB, Xu JJ and Smolarek TA (2005) Differential interaction of 3-hydroxy-3-methylglutaryl-coa reductase inhibitors with ABCB1, ABCC2, and OATP1B1. *Drug Metab Dispos* 33(4):537-546.
- Chung JY, Cho JY, Yu KS, Kim JR, Oh DS, Jung HR, Lim KS, Moon KH, Shin SG and Jang IJ (2005) Effect of OATP1B1 (SLCO1B1) variant alleles on the pharmacokinetics of pitavastatin in healthy volunteers. *Clin Pharmacol Ther* 78(4):342-350.
- Cziraky MJ, Willey VJ, McKenney JM, Kamat SA, Fisher MD, Guyton JR, Jacobson TA and Davidson MH (2006) Statin safety: an assessment using an administrative claims database. *Am J Cardiol* 97(8A):61C-68C.
- Davidson AL and Maloney PC (2007) ABC transporters: how small machines do a big job. *Trends Microbiol* 15(10):448-455.
- Fujino H, Nakai D, Nakagomi R, Saito M, Tokui T and Kojima J (2004) Metabolic stability and uptake by human hepatocytes of pitavastatin, a new inhibitor of HMG-CoA reductase. *Arzneimittelforschung* 54(7):382-388.
- Giacomini KM and Sugiyama Y (2006) Membrane Transporters and Drug Response, in *Goodman & Gilman's The Pharmacological Basis of Therapeutics* (Brunton LL, Lazo JS and Parker KL eds) pp 41-70, McGraw-Hill Companies, New York.
- Gonzales FJ and Tukey RH (2006) Drug Metabolism, in *Goodman & Gilman's The Pharmacological Basis of Therapeutics* (Brunton LL, Lazo JS and Parker KL eds) pp 71-91, McGraw-Hill Companies, New York.

- Graham DJ, Staffa JA, Shatin D, Andrade SE, Schech SD, La Grenade L, Gurwitz JH, Chan KA, Goodman MJ and Platt R (2004) Incidence of hospitalized rhabdomyolysis in patients treated with lipid-lowering drugs. *Jama* 292(21):2585-2590.
- Hagenbuch B and Meier PJ (2004) Organic anion transporting polypeptides of the OATP/SLC21 family: phylogenetic classification as OATP/SLCO superfamily, new nomenclature and molecular/functional properties. *Pflugers Arch* 447(5):653-665.
- Hatanaka T (2000) Clinical pharmacokinetics of pravastatin: mechanisms of pharmacokinetic events. *Clin Pharmacokinet* 39(6):397-412.
- Hermann M, Asberg A, Christensen H, Holdaas H, Hartmann A and Reubsæet JL (2004) Substantially elevated levels of atorvastatin and metabolites in cyclosporine-treated renal transplant recipients. *Clin Pharmacol Ther* 76(4):388-391.
- Hermann M, Bogsrud MP, Molden E, Asberg A, Mohebi BU, Ose L and Retterstol K (2006) Exposure of atorvastatin is unchanged but lactone and acid metabolites are increased several-fold in patients with atorvastatin-induced myopathy. *Clin Pharmacol Ther* 79(6):532-539.
- Hirano M, Maeda K, Hayashi H, Kusuhara H and Sugiyama Y (2005) Bile salt export pump (BSEP/ABCB11) can transport a nonbile acid substrate, pravastatin. *J Pharmacol Exp Ther* 314(2):876-882.
- Ho RH and Kim RB (2005) Transporters and drug therapy: implications for drug disposition and disease. *Clin Pharmacol Ther* 78(3):260-277.
- Hsiang B, Zhu Y, Wang Z, Wu Y, Sasseville V, Yang WP and Kirchgessner TG (1999) A novel human hepatic organic anion transporting polypeptide (OATP2). Identification of a liver-specific human organic anion transporting polypeptide and identification of rat and human hydroxymethylglutaryl-CoA reductase inhibitor transporters. *J Biol Chem* 274(52):37161-37168.
- Ishigami M, Honda T, Takasaki W, Ikeda T, Komai T, Ito K and Sugiyama Y (2001) A comparison of the effects of 3-hydroxy-3-methylglutaryl-coenzyme a (HMG-CoA) reductase inhibitors on the CYP3A4-dependent oxidation of mexazolam in vitro. *Drug Metab Dispos* 29(3):282-288.
- Iwai M, Suzuki H, Ieiri I, Otsubo K and Sugiyama Y (2004) Functional analysis of single nucleotide polymorphisms of hepatic organic anion transporter OATP1B1 (OATP-C). *Pharmacogenetics* 14(11):749-757.
- Kakyo M, Sakagami H, Nishio T, Nakai D, Nakagomi R, Tokui T, Naitoh T, Matsuno S, Abe T and Yawo H (1999) Immunohistochemical distribution and functional characterization of an organic anion transporting polypeptide 2 (oatp2). *FEBS Lett* 445(2-3):343-346.
- Kameyama Y, Yamashita K, Kobayashi K, Hosokawa M and Chiba K (2005) Functional characterization of SLCO1B1 (OATP-C) variants, SLCO1B1*5, SLCO1B1*15 and SLCO1B1*15+C1007G, by using transient expression systems of HeLa and HEK293 cells. *Pharmacogenet Genomics* 15(7):513-522.
- Kantola T, Kivisto KT and Neuvonen PJ (1998a) Effect of itraconazole on the pharmacokinetics of atorvastatin. *Clin Pharmacol Ther* 64(1):58-65.
- Kantola T, Kivisto KT and Neuvonen PJ (1998b) Erythromycin and verapamil considerably increase serum simvastatin and simvastatin acid concentrations. *Clin Pharmacol Ther* 64(2):177-182.
- Kim RB (2006) Transporters and drug discovery: why, when, and how. *Mol Pharm* 3(1):26-32.
- Knoll RW, Ciafone R and Galen M (1993) Rhabdomyolysis and renal failure secondary to combination therapy of hyperlipidemia with lovastatin and gemfibozil. *Conn Med* 57(9):593-594.

- Kobayashi D, Nozawa T, Imai K, Nezu J, Tsuji A and Tamai I (2003) Involvement of human organic anion transporting polypeptide OATP-B (SLC21A9) in pH-dependent transport across intestinal apical membrane. *J Pharmacol Exp Ther* 306(2):703-708.
- Konig J, Cui Y, Nies AT and Keppler D (2000) A novel human organic anion transporting polypeptide localized to the basolateral hepatocyte membrane. *Am J Physiol Gastrointest Liver Physiol* 278(1):G156-164.
- Konig J, Seithel A, Gradhand U and Fromm MF (2006) Pharmacogenomics of human OATP transporters. *Naunyn Schmiedebergs Arch Pharmacol* 372(6):432-443.
- Kruh J (1982) Effects of sodium butyrate, a new pharmacological agent, on cells in culture. *Mol Cell Biochem* 42(2):65-82.
- Kyrklund C, Backman JT, Neuvonen M and Neuvonen PJ (2003) Gemfibrozil increases plasma pravastatin concentrations and reduces pravastatin renal clearance. *Clin Pharmacol Ther* 73(6):538-544.
- Lau YY, Huang Y, Frassetto L and Benet LZ (2007) Effect of OATP1B transporter inhibition on the pharmacokinetics of atorvastatin in healthy volunteers. *Clin Pharmacol Ther* 81(2):194-204.
- Lau YY, Okochi H, Huang Y and Benet LZ (2006) Multiple transporters affect the disposition of atorvastatin and its two active hydroxy metabolites: application of in vitro and ex situ systems. *J Pharmacol Exp Ther* 316(2):762-771.
- Lau YY, Wu CY, Okochi H and Benet LZ (2004) Ex situ inhibition of hepatic uptake and efflux significantly changes metabolism: hepatic enzyme-transporter interplay. *J Pharmacol Exp Ther* 308(3):1040-1045.
- Le Vee M, Jigorel E, Glaise D, Gripon P, Guguen-Guillouzo C and Fardel O (2006) Functional expression of sinusoidal and canalicular hepatic drug transporters in the differentiated human hepatoma HepaRG cell line. *Eur J Pharm Sci* 28(1-2):109-117.
- Lee E, Ryan S, Birmingham B, Zalikowski J, March R, Ambrose H, Moore R, Lee C, Chen Y and Schneck D (2005) Rosuvastatin pharmacokinetics and pharmacogenetics in white and Asian subjects residing in the same environment. *Clin Pharmacol Ther* 78(4):330-341.
- Lennernas H (2003) Clinical pharmacokinetics of atorvastatin. *Clin Pharmacokinet* 42(13):1141-1160.
- Louis M, Rosato RR, Brault L, Osbild S, Battaglia E, Yang XH, Grant S and Bagrel D (2004) The histone deacetylase inhibitor sodium butyrate induces breast cancer cell apoptosis through diverse cytotoxic actions including glutathione depletion and oxidative stress. *Int J Oncol* 25(6):1701-1711.
- Lowry OH, Rosebrough NJ, Farr AL and Randall RJ (1951) Protein measurement with the Folin phenol reagent. *J Biol Chem* 193(1):265-275.
- Maeda K, Ieiri I, Yasuda K, Fujino A, Fujiwara H, Otsubo K, Hirano M, Watanabe T, Kitamura Y, Kusuhara H and Sugiyama Y (2006) Effects of organic anion transporting polypeptide 1B1 haplotype on pharmacokinetics of pravastatin, valsartan, and temocapril. *Clin Pharmacol Ther* 79(5):427-439.
- Markwell MA, Haas SM, Bieber LL and Tolbert NE (1978) A modification of the Lowry procedure to simplify protein determination in membrane and lipoprotein samples. *Anal Biochem* 87(1):206-210.
- Marzolini C, Tirona RG and Kim RB (2004) Pharmacogenomics of the OATP and OAT families. *Pharmacogenomics* 5(3):273-282.

Matsushima S, Maeda K, Kondo C, Hirano M, Sasaki M, Suzuki H and Sugiyama Y (2005) Identification of the hepatic efflux transporters of organic anions using double-transfected Madin-Darby canine kidney II cells expressing human organic anion-transporting polypeptide 1B1 (OATP1B1)/multidrug resistance-associated protein 2, OATP1B1/multidrug resistance 1, and OATP1B1/breast cancer resistance protein. *J Pharmacol Exp Ther* 314(3):1059-1067.

Maxa JL, Melton LB, Ogu CC, Sills MN and Limanni A (2002) Rhabdomyolysis after concomitant use of cyclosporine, simvastatin, gemfibrozil, and itraconazole. *Ann Pharmacother* 36(5):820-823.

McTaggart F, Buckett L, Davidson R, Holdgate G, McCormick A, Schneck D, Smith G and Warwick M (2001) Preclinical and clinical pharmacology of Rosuvastatin, a new 3-hydroxy-3-methylglutaryl coenzyme A reductase inhibitor. *Am J Cardiol* 87(5A):28B-32B.

Meier PJ, Eckhardt U, Schroeder A, Hagenbuch B and Stieger B (1997) Substrate specificity of sinusoidal bile acid and organic anion uptake systems in rat and human liver. *Hepatology* 26(6):1667-1677.

Michalski C, Cui Y, Nies AT, Nuessler AK, Neuhaus P, Zanger UM, Klein K, Eichelbaum M, Keppler D and Konig J (2002) A naturally occurring mutation in the SLC21A6 gene causing impaired membrane localization of the hepatocyte uptake transporter. *J Biol Chem* 277(45):43058-43063.

Morimoto K, Oishi T, Ueda S, Ueda M, Hosokawa M and Chiba K (2004) A novel variant allele of OATP-C (SLCO1B1) found in a Japanese patient with pravastatin-induced myopathy. *Drug Metab Pharmacokinet* 19(6):453-455.

Mwinyi J, Johne A, Bauer S, Roots I and Gerloff T (2004) Evidence for inverse effects of OATP-C (SLC21A6) 5 and 1b haplotypes on pravastatin kinetics. *Clin Pharmacol Ther* 75(5):415-421.

Nakagomi-Hagihara R, Nakai D, Tokui T, Abe T and Ikeda T (2007) Gemfibrozil and its glucuronide inhibit the hepatic uptake of pravastatin mediated by OATP1B1. *Xenobiotica* 37(5):474-486.

Nakai D, Nakagomi R, Furuta Y, Tokui T, Abe T, Ikeda T and Nishimura K (2001) Human liver-specific organic anion transporter, LST-1, mediates uptake of pravastatin by human hepatocytes. *J Pharmacol Exp Ther* 297(3):861-867.

Neuvonen PJ and Jalava KM (1996) Itraconazole drastically increases plasma concentrations of lovastatin and lovastatin acid. *Clin Pharmacol Ther* 60(1):54-61.

Nezasa K, Higaki K, Takeuchi M, Nakano M and Koike M (2003) Uptake of rosuvastatin by isolated rat hepatocytes: comparison with pravastatin. *Xenobiotica* 33(4):379-388.

Niemi M, Neuvonen PJ, Hofmann U, Backman JT, Schwab M, Lutjohann D, von Bergmann K, Eichelbaum M and Kivisto KT (2005) Acute effects of pravastatin on cholesterol synthesis are associated with SLCO1B1 (encoding OATP1B1) haplotype *17. *Pharmacogenet Genomics* 15(5):303-309.

Niemi M, Schaeffeler E, Lang T, Fromm MF, Neuvonen M, Kyrklund C, Backman JT, Kerb R, Schwab M, Neuvonen PJ, Eichelbaum M and Kivisto KT (2004) High plasma pravastatin concentrations are associated with single nucleotide polymorphisms and haplotypes of organic anion transporting polypeptide-C (OATP-C, SLCO1B1). *Pharmacogenetics* 14(7):429-440.

Nishizato Y, Ieiri I, Suzuki H, Kimura M, Kawabata K, Hirota T, Takane H, Irie S, Kusahara H, Urasaki Y, Urae A, Higuchi S, Otsubo K and Sugiyama Y (2003) Polymorphisms of OATP-C (SLC21A6) and OAT3 (SLC22A8) genes: consequences for pravastatin pharmacokinetics. *Clin Pharmacol Ther* 73(6):554-565.

Noe J, Portmann R, Brun ME and Funk C (2007) Substrate Dependent Drug-Drug Interactions between Gemfibrozil, Fluvastatin and Other Oatp Substrates on Oatp1b1, Oatp2b1 and Oatp1b3. *Drug Metab Dispos*.

- Nozawa T, Nakajima M, Tamai I, Noda K, Nezu J, Sai Y, Tsuji A and Yokoi T (2002) Genetic polymorphisms of human organic anion transporters OATP-C (SLC21A6) and OATP-B (SLC21A9): allele frequencies in the Japanese population and functional analysis. *J Pharmacol Exp Ther* 302(2):804-813.
- Omar MA, Wilson JP and Cox TS (2001) Rhabdomyolysis and HMG-CoA reductase inhibitors. *Ann Pharmacother* 35(9):1096-1107.
- Pasanen MK, Backman JT, Neuvonen PJ and Niemi M (2006) Frequencies of single nucleotide polymorphisms and haplotypes of organic anion transporting polypeptide 1B1 SLCO1B1 gene in a Finnish population. *Eur J Clin Pharmacol* 62(6):409-415.
- Pasanen MK, Fredrikson H, Neuvonen PJ and Niemi M (2007) Different Effects of SLCO1B1 Polymorphism on the Pharmacokinetics of Atorvastatin and Rosuvastatin. *Clin Pharmacol Ther* 82(6):726-733.
- Pierce LR, Wysowski DK and Gross TP (1990) Myopathy and rhabdomyolysis associated with lovastatin-gemfibrozil combination therapy. *Jama* 264(1):71-75.
- Pogson GW, Kindred LH and Carper BG (1999) Rhabdomyolysis and renal failure associated with cerivastatin-gemfibrozil combination therapy. *Am J Cardiol* 83(7):1146.
- Prueksaritanont T, Zhao JJ, Ma B, Roadcap BA, Tang C, Qiu Y, Liu L, Lin JH, Pearson PG and Baillie TA (2002) Mechanistic studies on metabolic interactions between gemfibrozil and statins. *J Pharmacol Exp Ther* 301(3):1042-1051.
- Regazzi MB, Iacona I, Campana C, Raddato V, Lesi C, Perani G, Gavazzi A and Vigano M (1993) Altered disposition of pravastatin following concomitant drug therapy with cyclosporin A in transplant recipients. *Transplant Proc* 25(4):2732-2734.
- Rohrbacher M, Kirchhof A, Skarke C, Geisslinger G and Lotsch J (2006) Rapid identification of three functionally relevant polymorphisms in the OATP1B1 transporter gene using Pyrosequencing. *Pharmacogenomics* 7(2):167-176.
- Sasaki M, Suzuki H, Aoki J, Ito K, Meier PJ and Sugiyama Y (2004) Prediction of in vivo biliary clearance from the in vitro transcellular transport of organic anions across a double-transfected Madin-Darby canine kidney II monolayer expressing both rat organic anion transporting polypeptide 4 and multidrug resistance associated protein 2. *Mol Pharmacol* 66(3):450-459.
- Sasaki M, Suzuki H, Ito K, Abe T and Sugiyama Y (2002) Transcellular transport of organic anions across a double-transfected Madin-Darby canine kidney II cell monolayer expressing both human organic anion-transporting polypeptide (OATP2/SLC21A6) and Multidrug resistance-associated protein 2 (MRP2/ABCC2). *J Biol Chem* 277(8):6497-6503.
- Schindler C, Thorns M, Matschke K, Tugtekin SM and Kirch W (2007) Asymptomatic statin-induced rhabdomyolysis after long-term therapy with the hydrophilic drug pravastatin. *Clin Ther* 29(1):172-176.
- Schneck DW, Birmingham BK, Zalikowski JA, Mitchell PD, Wang Y, Martin PD, Lasseter KC, Brown CD, Windass AS and Raza A (2004) The effect of gemfibrozil on the pharmacokinetics of rosuvastatin. *Clin Pharmacol Ther* 75(5):455-463.
- Seithel A, Eberl S, Singer K, Auge D, Heinkele G, Wolf NB, Dorje F, Fromm MF and Konig J (2007) The influence of macrolide antibiotics on the uptake of organic anions and drugs mediated by OATP1B1 and OATP1B3. *Drug Metab Dispos*.
- Shitara Y, Hirano M, Adachi Y, Itoh T, Sato H and Sugiyama Y (2004a) In vitro and in vivo correlation of the inhibitory effect of cyclosporin A on the transporter-mediated hepatic uptake of cerivastatin in rats. *Drug Metab Dispos* 32(12):1468-1475.
- Shitara Y, Hirano M, Sato H and Sugiyama Y (2004b) Gemfibrozil and its glucuronide inhibit the organic anion transporting polypeptide 2 (OATP2/OATP1B1:SLC21A6)-mediated hepatic uptake and CYP2C8-mediated metabolism of cerivastatin: analysis of the mechanism of the

- clinically relevant drug-drug interaction between cerivastatin and gemfibrozil. *J Pharmacol Exp Ther* 311(1):228-236.
- Shitara Y, Itoh T, Sato H, Li AP and Sugiyama Y (2003a) Inhibition of transporter-mediated hepatic uptake as a mechanism for drug-drug interaction between cerivastatin and cyclosporin A. *J Pharmacol Exp Ther* 304(2):610-616.
- Shitara Y, Li AP, Kato Y, Lu C, Ito K, Itoh T and Sugiyama Y (2003b) Function of uptake transporters for taurocholate and estradiol 17 β -D-glucuronide in cryopreserved human hepatocytes. *Drug Metab Pharmacokinet* 18(1):33-41.
- Shitara Y, Sato H and Sugiyama Y (2005) Evaluation of drug-drug interaction in the hepatobiliary and renal transport of drugs. *Annu Rev Pharmacol Toxicol* 45:689-723.
- Shitara Y and Sugiyama Y (2006) Pharmacokinetic and pharmacodynamic alterations of 3-hydroxy-3-methylglutaryl coenzyme A (HMG-CoA) reductase inhibitors: drug-drug interactions and interindividual differences in transporter and metabolic enzyme functions. *Pharmacol Ther* 112(1):71-105.
- Smith NF, Figg WD and Sparreboom A (2005) Role of the liver-specific transporters OATP1B1 and OATP1B3 in governing drug elimination. *Expert Opin Drug Metab Toxicol* 1(3):429-445.
- Tachibana-Iimori R, Tabara Y, Kusuhara H, Kohara K, Kawamoto R, Nakura J, Tokunaga K, Kondo I, Sugiyama Y and Miki T (2004) Effect of genetic polymorphism of OATP-C (SLCO1B1) on lipid-lowering response to HMG-CoA reductase inhibitors. *Drug Metab Pharmacokinet* 19(5):375-380.
- Tal A, Rajeshawari M and Isley W (1997) Rhabdomyolysis associated with simvastatin-gemfibrozil therapy. *South Med J* 90(5):546-547.
- Thomas P and Smart TG (2005) HEK293 cell line: a vehicle for the expression of recombinant proteins. *J Pharmacol Toxicol Methods* 51(3):187-200.
- Thompson PD, Clarkson P and Karas RH (2003) Statin-associated myopathy. *Jama* 289(13):1681-1690.
- Tian X, Zamek-Gliszczynski MJ, Zhang P and Brouwer KL (2004) Modulation of multidrug resistance-associated protein 2 (Mrp2) and Mrp3 expression and function with small interfering RNA in sandwich-cultured rat hepatocytes. *Mol Pharmacol* 66(4):1004-1010.
- Tian X, Zhang P, Zamek-Gliszczynski MJ and Brouwer KL (2005) Knocking down transport: applications of RNA interference in the study of drug transport proteins. *Drug Metab Rev* 37(4):705-723.
- Tirona RG, Leake BF, Merino G and Kim RB (2001) Polymorphisms in OATP-C: identification of multiple allelic variants associated with altered transport activity among European- and African-Americans. *J Biol Chem* 276(38):35669-35675.
- Tirona RG, Leake BF, Wolkoff AW and Kim RB (2003) Human organic anion transporting polypeptide-C (SLC21A6) is a major determinant of rifampin-mediated pregnane X receptor activation. *J Pharmacol Exp Ther* 304(1):223-228.
- Ware JA (2006) Membrane transporters in drug discovery and development: A new mechanistic ADME era. *Mol Pharm* 3(1):1-2.
- Yamazaki M, Akiyama S, Nishigaki R and Sugiyama Y (1996) Uptake is the rate-limiting step in the overall hepatic elimination of pravastatin at steady-state in rats. *Pharm Res* 13(10):1559-1564.
- Yamazaki M, Li B, Louie SW, Pudvah NT, Stocco R, Wong W, Abramovitz M, Demartis A, Laufer R, Hochman JH, Prueksaritanont T and Lin JH (2005) Effects of fibrates on human organic anion-transporting polypeptide 1B1-, multidrug resistance protein 2- and P-glycoprotein-mediated transport. *Xenobiotica* 35(7):737-753.

Yamazaki M, Suzuki H, Hanano M, Tokui T, Komai T and Sugiyama Y (1993) Na(+)-independent multispecific anion transporter mediates active transport of pravastatin into rat liver. *Am J Physiol* 264(1 Pt 1):G36-44.

Zhang L, Strong JM, Qiu W, Lesko LJ and Huang SM (2006) Scientific perspectives on drug transporters and their role in drug interactionst. *Mol Pharm* 3(1):62-69.

Åsberg A, Hartmann A, Fjeldsa E, Bergan S and Holdaas H (2001) Bilateral pharmacokinetic interaction between cyclosporine A and atorvastatin in renal transplant recipients. *Am J Transplant* 1(4):382-386.

7 APPENDIX

7.1 Appendix 1

Results from experiments on HEK293 cells using cell culturing conditions different from the conditions described in chapter 2.2.1:

Culture medium: 500 ml D-MEM/F-12 (1:1) (1x) liquid with GlutaMAX™ I, 50 ml heat inactivated FCS, 2.5 ml PEST and 5 ml Geneticin (50 mg/ml) was used.

Splitting: 1 million cells in 75 cm² flasks with 25 ml culture medium, grown for 7 days before new splitting/seeding.

Trypsinated: No

Seeding density: 0.5 million cells/well, 24-well plates

Cells: AstraZeneca R&D Mölndal (AstraZeneca Alderley Park)

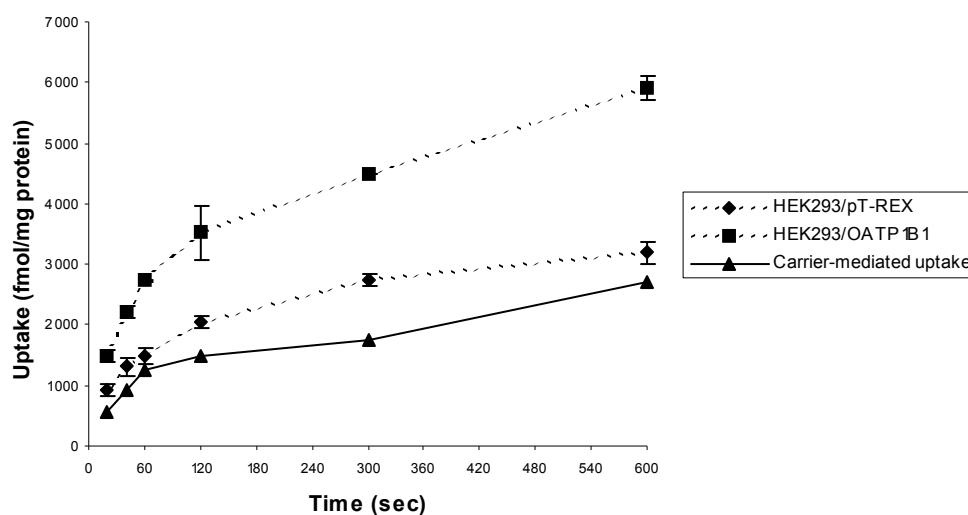


Figure 7.1 Time course of [³H]atorvastatin (80 nM, 0.4 μ Ci/ml) uptake in HEK293 cells transfected with OATP1B1 (■) and vector-transfected control cells, HEK293/pT-REX (◆). The triangles (▲) represent the carrier-mediated uptake in the OATP1B1-expressing HEK293 cells. Each point represents the mean \pm S.D. (n=3).

7.2 Appendix 2

Results from experiments on HEK293 cells using cell culturing conditions different from the conditions described in chapter 2.2.1:

Culture medium: 500 ml D-MEM/F-12 (1:1) (1x) liquid with GlutaMAX™ I, 50 ml heat inactivated FCS, 2.5 ml PEST and 5 ml Geneticin (50 mg/ml) was used.

Splitting: 1 million cells in 75 cm² flasks with 25 ml culture medium, grown for 7 days before new splitting/seeding.

Trypsinated: No

Seeding density: 0.5 million cells/well, 24-well plates

Cells: AstraZeneca R&D Mölndal (AstraZeneca Alderley Park)

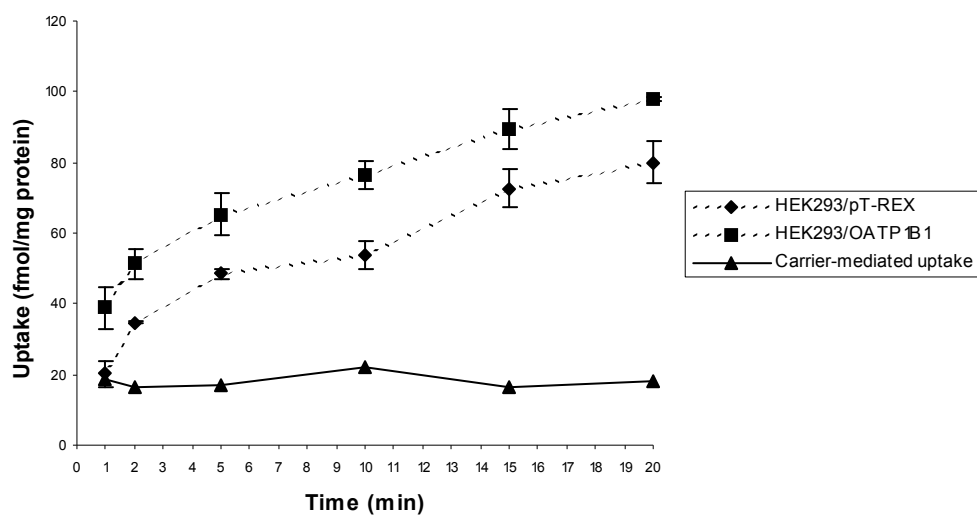


Figure 7.2 Time course of [³H]pravastatin (50 nM, 1 μ Ci/ml) uptake in HEK293 cells transfected with OATP1B1 (■) and vector-transfected control cells, HEK293/pT-REX (◆). The triangles (▲) represent the carrier-mediated uptake in the OATP1B1-expressing HEK293 cells. Each point represents the mean \pm S.D. (n=3).

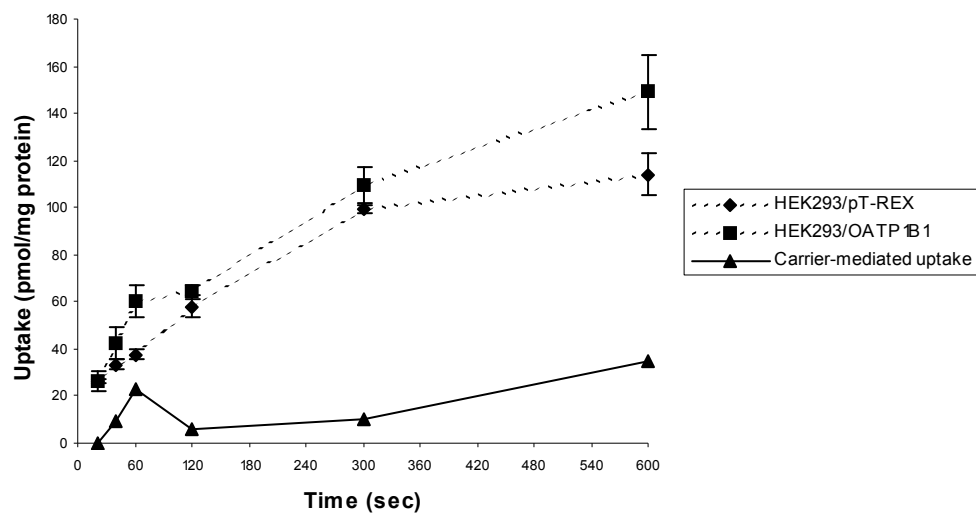


Figure 7.3 Time course of [³H]pravastatin (50 μ M, 1 μ Ci/ml) uptake in HEK293 cells transfected with OATP1B1 (■) and vector-transfected control cells, HEK293/pT-REX (◆). The triangles (▲) represent the carrier-mediated uptake in the OATP1B1-expressing HEK293 cells. Each point represents the mean \pm S.D. (n=3).

Results from experiments on HEK293 cells using cell culturing conditions different from the conditions described in chapter 2.2.1:

Culture medium: 500 ml D-MEM/F-12 (1:1) (1x) liquid with GlutaMAX™ I, 50 ml heat inactivated FCS, 2.5 ml PEST and 5 ml Geneticin (50 mg/ml) was used.

Splitting: 1 million cells in 75 cm² flasks with 25 ml culture medium, grown for 7 days before new splitting/seeding.

Trypsinated: No

Seeding density: 0.5 million cells/well, 24-well plates

Cells: AstraZeneca R&D Mölndal (AstraZeneca Alderley Park)

Sodium butyrate: The cells seeded in 24-well plates were treated with 10 µM Na-butyrate 24 hours prior to experimentation.

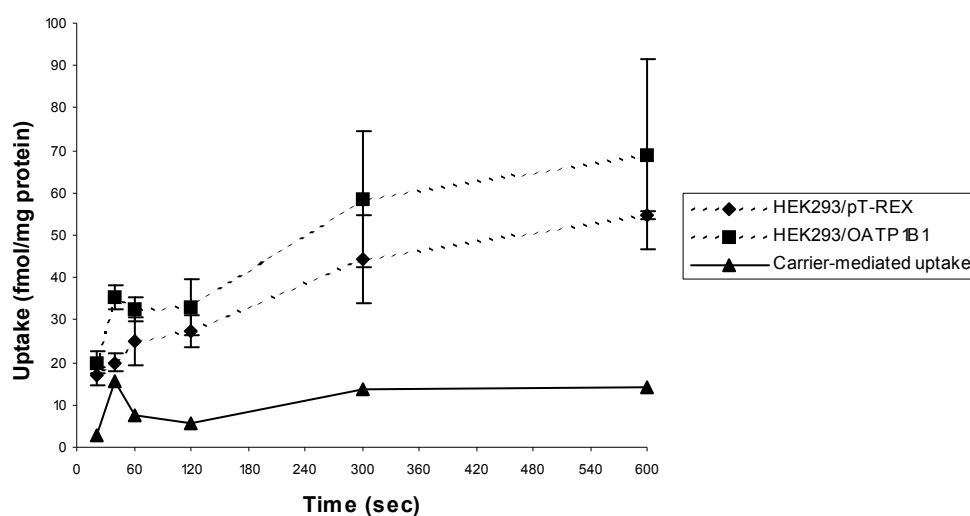


Figure 7.4 Time course of [³H]pravastatin (50 nM, 1 µCi/ml) uptake in HEK293 cells transfected with OATP1B1 (■) and vector-transfected control cells, HEK293/pT-REX (◆). The triangles (▲) represent the carrier-mediated uptake in the OATP1B1-expressing HEK293 cells. Each point represents the mean ± S.D. (n=3).

7.3 Appendix 3

Results from experiments on HEK293 cells using cell culturing conditions different from the conditions described in chapter 2.2.1:

Culture medium: 500 ml D-MEM/F-12 (1:1) (1x) liquid with GlutaMAX™ I, 50 ml heat inactivated FCS, 2.5 ml PEST and 5 ml Geneticin (50 mg/ml) was used.

Splitting: 1 million cells in 75 cm² flasks with 25 ml culture medium, grown for 7 days before new splitting/seeding.

Trypsinated: No

Seeding density: 0.5 million cells/well, 24-well plates

Cells: AstraZeneca R&D Mölndal (AstraZeneca Alderley Park)

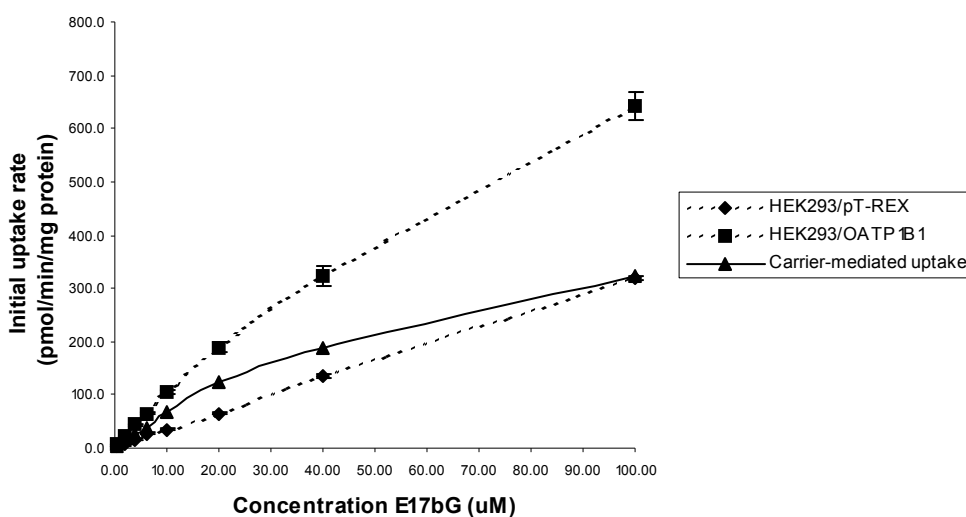


Figure 7.5 Concentration dependence of the initial uptake rate of estradiol-17β-D-glucuronide (0.53-100 μM, 1.59 μCi/ml) in HEK293 cells transfected with OATP1B1 (■) and vector-transfected control cells, HEK293/pT-REX (♦). The triangles (▲) represent the carrier-mediated uptake in the OATP1B1-expressing HEK293 cells. Each point represents the mean ± S.D. (n=3).

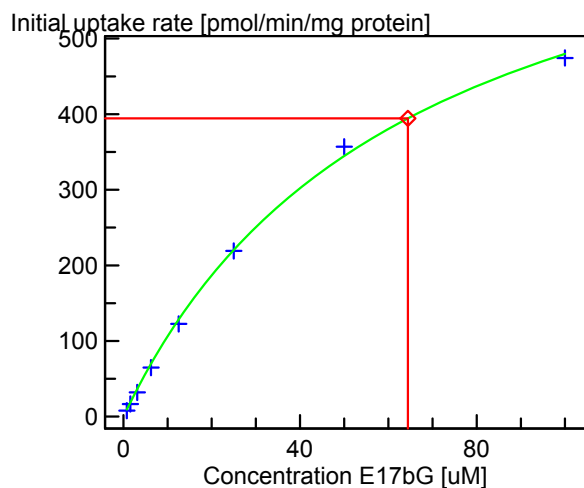


Figure 7.6 The carrier-mediated uptake of estradiol-17 β -D-glucuronide in HEK293/OATP1B1 cells after fitting the uptake data to the modified Michaelis-Menten model (Equation 1.4). The dotted line expresses the estimation of the K_m value; the substrate concentration at $\frac{1}{2} V_{max}$ (Figure 1.8). Kinetic analysis estimated K_m and V_{max} values of $77.4 \pm 4.6 \mu\text{M}$ and $570.7 \pm 19.0 \text{ pmol/min/mg protein}$, respectively.

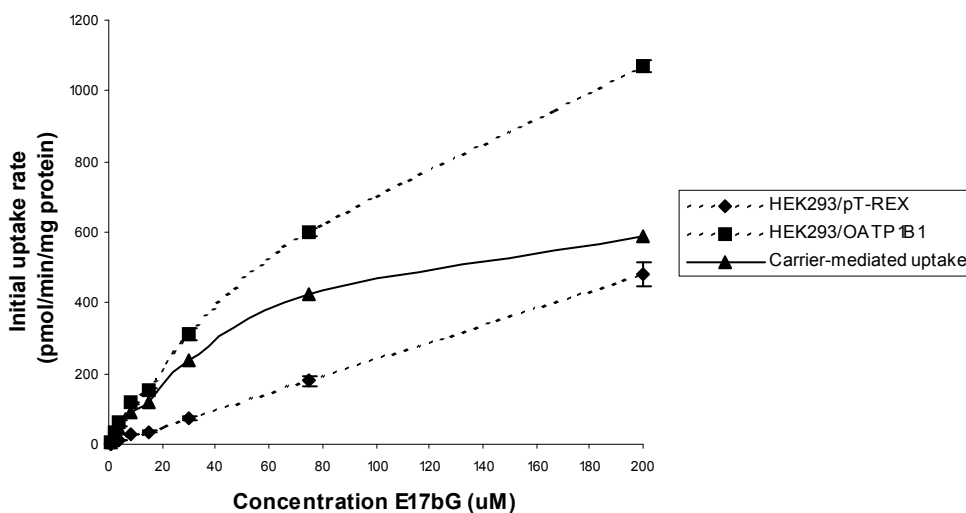


Figure 7.7 Concentration dependence of the initial uptake rate of estradiol-17 β -D-glucuronide (0.5-200 μM , 1.06 $\mu\text{Ci/ml}$) in HEK293 cells transfected with OATP1B1 (\blacksquare) and vector-transfected control cells, Hek293/pT-REX (\blacklozenge). The triangles (\blacktriangle) represent the carrier-mediated uptake in the OATP1B1-expressing HEK293 cells. Each point represents the mean \pm S.D. ($n=3$).

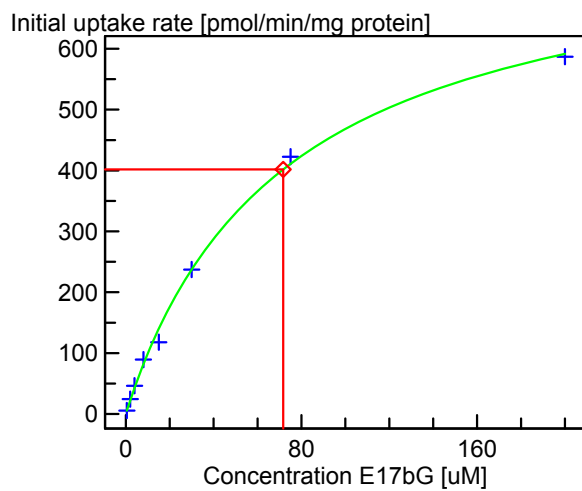


Figure 7.8 The carrier-mediated uptake of estradiol-17β-D-glucuronide in HEK293/OATP1B1 cells after fitting the uptake data to the modified Michaelis-Menten model (Equation 1.4). The dotted line expresses the estimation of the K_m value; the substrate concentration at $\frac{1}{2} V_{max}$ (Figure 1.8). Kinetic analysis estimated K_m and V_{max} values of $71.7 \pm 5.6 \mu\text{M}$ and $803.6 \pm 27.4 \text{ pmol/min/mg protein}$, respectively.

Results from experiments on HEK293 cells using cell culturing conditions different from the conditions described in chapter 2.2.1:

Laboratory: The experiments were performed at AstraZeneca R&D Lund with cells grown and seeded there.

Cells: AstraZeneca R&D Lund

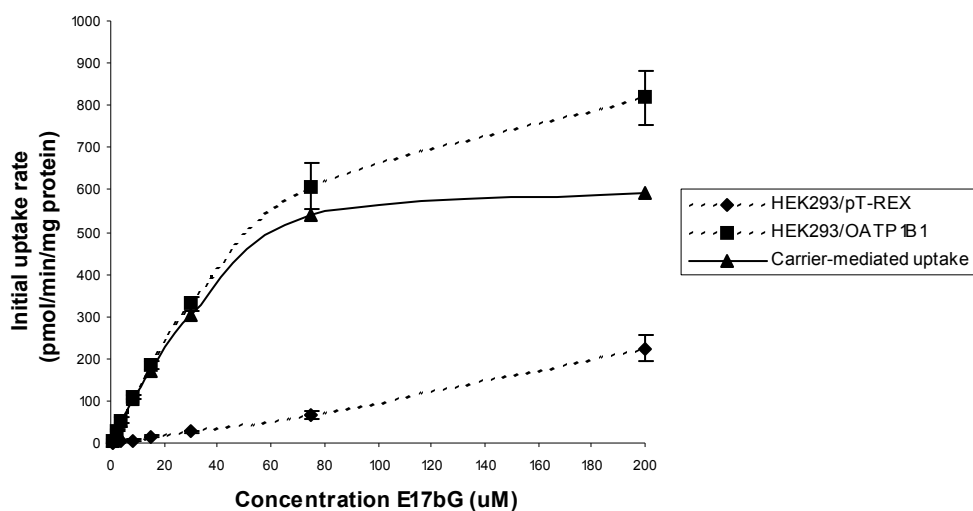


Figure 7.9 Concentration dependence of the initial uptake rate of estradiol-17 β -D-glucuronide (0.5-200 μ M, 1.06 μ Ci/ml) in HEK293 cells transfected with OATP1B1 (\blacksquare) and vector-transfected control cells, HEK293/pT-REX (\blacklozenge). The triangles (\blacktriangle) represent the carrier-mediated uptake in the OATP1B1-expressing HEK293 cells. Each point represents the mean \pm S.D. (n=3).

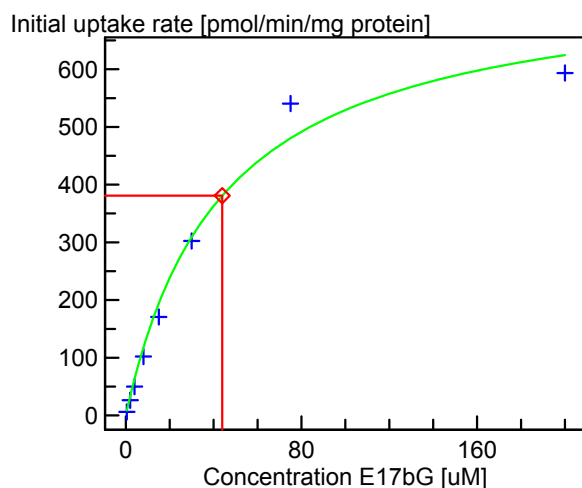


Figure 7.10 The carrier-mediated uptake of estradiol-17 β -D-glucuronide in HEK293/OATP1B1 cells after fitting the uptake data to the modified Michaelis-Menten model (Equation 1.4) The dotted line expresses the estimation of the K_m value; the substrate concentration at $\frac{1}{2} V_{max}$ (Figure 1.8). Kinetic analysis estimated K_m and V_{max} values of $43.9 \pm 8.1 \mu$ M and 761.6 ± 53.6 pmol/min/mg protein, respectively.

7.4 Appendix 4

Results from experiments on HEK293 cells using different amount of radioactive compound in the test solutions in the dilution series:

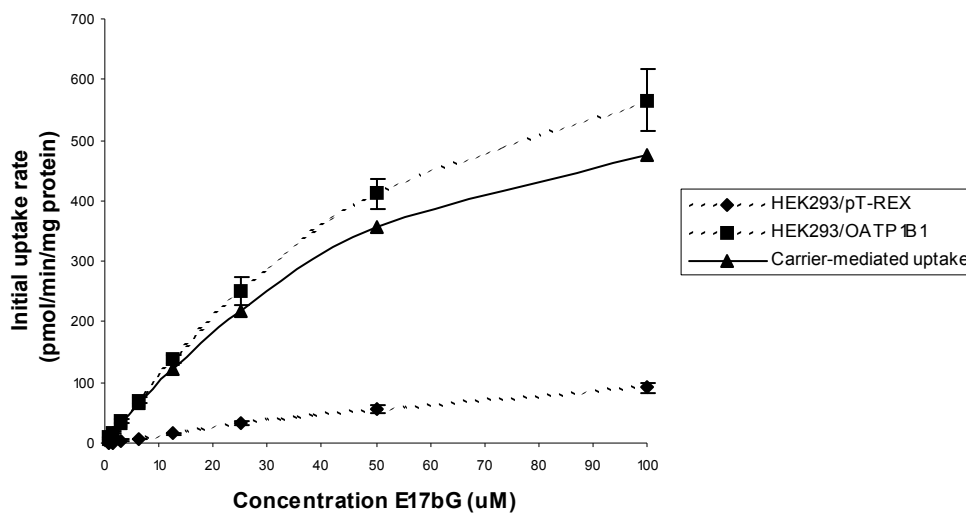


Figure 7.11 Concentration dependence of the initial uptake rate of estradiol-17 β -D-glucuronide (0.78-100 μ M, 0.037-4.69 μ Ci/ml) in HEK293 cells transfected with OATP1B1 (\blacksquare) and vector-transfected control cells, HEK293/pT-REX (\blacklozenge). The triangles (\blacktriangle) represent the carrier-mediated uptake in the OATP1B1-expressing HEK293 cells. Each point represents the mean \pm S.D. (n=3).

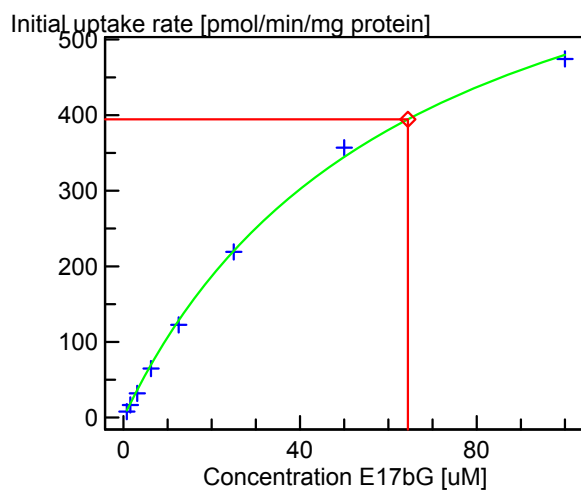


Figure 7.12 The carrier-mediated uptake of estradiol-17 β -D-glucuronide in HEK293/OATP1B1 cells after fitting the uptake data to the modified Michaelis-Menten model (Equation 1.4) The dotted line expresses the estimation of the K_m value; the substrate concentration at $\frac{1}{2} V_{max}$ (Figure 1.8). Kinetic analysis estimated K_m and V_{max} values of $64.4 \pm 4.6 \mu$ M and 788.8 ± 29.4 pmol/min/mg protein, respectively.

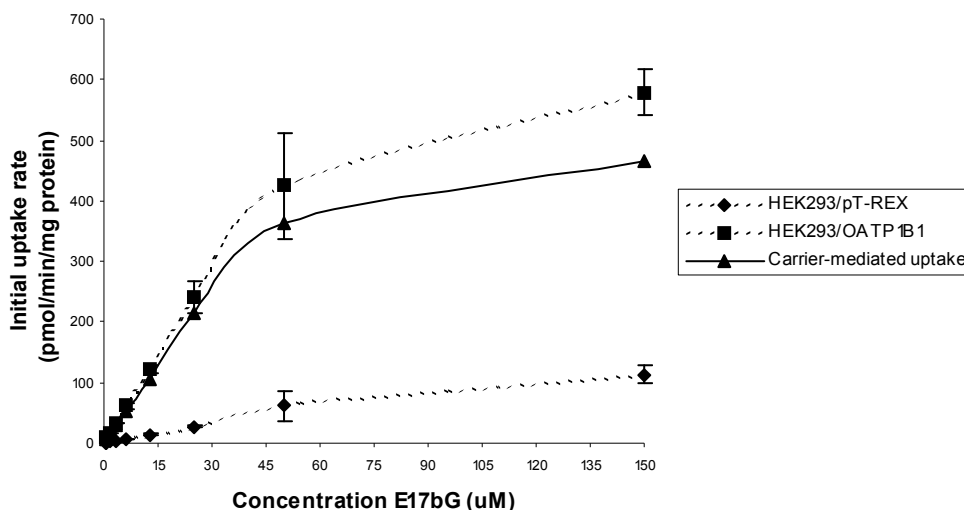


Figure 7.13 Concentration dependence of the initial uptake rate of estradiol-17 β -D-glucuronide (0.78-150 μ M, 0.037-7.035 μ Ci/ml) in HEK293 cells transfected with OATP1B1 (\blacksquare) and vector-transfected control cells, HEK293/pT-REX (\blacklozenge). The triangles (\blacktriangle) represent the carrier-mediated uptake in the OATP1B1-expressing HEK293 cells. Each point represents the mean \pm S.D. (n=3).

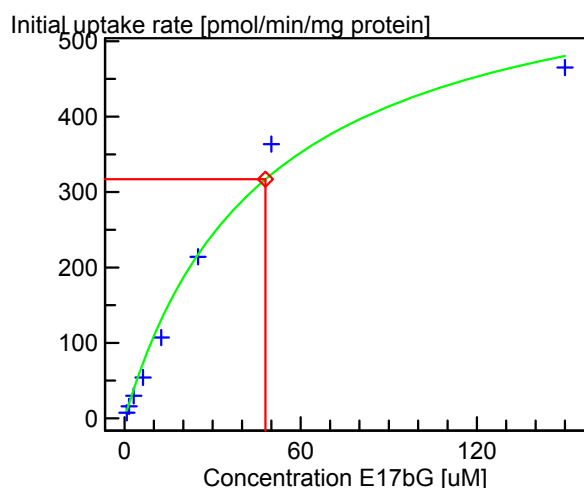


Figure 7.14 The carrier-mediated uptake of estradiol-17 β -D-glucuronide in HEK293/OATP1B1 cells after fitting the uptake data to the modified Michaelis-Menten model (Equation 1.4). The dotted line expresses the estimation of the K_m value; the substrate concentration at $\frac{1}{2} V_{max}$ (Figure 1.8). Kinetic analysis estimated K_m and V_{max} values of $48.0 \pm 8.8 \mu$ M and $634.1 \pm 50.3 \text{ pmol/min/mg protein}$, respectively.